Biochemical and Biophysical Research Communications 460 (2015) 5–21

Contents lists available at ScienceDirect

Biochemical and Biophysical Research Communications

journal homepage: www.elsevier.com/locate/ybbrc

Review

# Calmodulin and STIM proteins: Two major calcium sensors in the cytoplasm and endoplasmic reticulum

Christopher B. Marshall [a], Tadateru Nishikawa [a], Masanori Osawa [b], Peter B. Stathopulos [c, *], Mitsuhiko Ikura [a, *]

[a] Princess Margaret Cancer Centre, University Health Network and University of Toronto, Toronto, Ontario, M5G 1L7, Canada
[b] Graduate School of Pharmaceutical Sciences, The University of Tokyo, Hongo, Tokyo, 113-0033, Japan
[c] Department of Physiology and Pharmacology, Schulich School of Medicine and Dentistry, University of Western Ontario, London, Ontario, N6A 5C1, Canada

ARTICLE INFO

*Article history:*
Received 6 January 2015
Available online 18 May 2015

In memory of Professor Koichi Yagi, Hokkaido University.

*Keywords:*
Calmodulin
Stromal interaction molecules (STIM)
EF-hand
Calcium sensing
Atomic resolution structure
Calmodulin target interactions

ABSTRACT

The calcium ($Ca^{2+}$) ion is a universal signalling messenger which plays vital physiological roles in all eukaryotes. To decode highly regulated intracellular $Ca^{2+}$ signals, cells have evolved a number of sensor proteins that are ideally adapted to respond to a specific range of $Ca^{2+}$ levels. Among many such proteins, calmodulin (CaM) is a multi-functional cytoplasmic $Ca^{2+}$ sensor with a remarkable ability to interact with and regulate a plethora of structurally diverse target proteins. CaM achieves this 'multi-talented' functionality through two EF-hand domains, each with an independent capacity to bind targets, and an adaptable flexible linker. By contrast, stromal interaction molecule-1 and -2 (STIMs) have evolved for a specific role in endoplasmic reticulum (ER) $Ca^{2+}$ sensing using EF-hand machinery analogous to CaM; however, whereas CaM structurally adjusts to dissimilar binding partners, STIMs use the EF-hand machinery to self-regulate the stability of the $Ca^{2+}$ sensing domain. The molecular mechanisms underlying the $Ca^{2+}$-dependent signal transduction by CaM and STIMs have revealed a remarkable repertoire of actions and underscore the flexibility of nature in molecular evolution and adaption to discrete $Ca^{2+}$ levels. Recent genomic sequencing efforts have uncovered a number of disease-associated mutations in both CaM and STIM1. This article aims to highlight the most recent key structural and functional findings in the CaM and STIM fields, and discusses how these two $Ca^{2+}$ sensor proteins execute their biological functions.



## 1. Introduction

It has been more than four decades since Cheung and Kakiuchi independently discovered a protein that regulates cyclic nucleotide phosphodiesterase (PDE) in the brain [1,2]. Importantly, Kakiuchi found that this regulator is responsible for conferring calcium ($Ca^{2+}$) dependency to the enzymatic activity of PDE. Hence, this relatively small (*i.e.* 16.7 kDa), heat-stable, acidic protein (*i.e.* pI ~4.5) was named initially $Ca^{2+}$-dependent regulator (CDR) and was later renamed calmodulin (CaM). In the early years of CaM research, it was rather surprising that a single protein stimulated several other proteins including adenylate cyclase [3], $Ca^{2+}$ adenosine triphosphatase (ATPase) [4,5], and myosin light chain kinase (MLCK) [6], all of which displayed $Ca^{2+}$ dependency, which required CaM. A fascinating finding was that both the synthesis and decomposition of the second messenger cyclic adenosine monophosphate (cAMP) is controlled by another second messenger, $Ca^{2+}$, *via* its interaction with CaM, which in turn activates the nucleotide processing enzymes, adenylate cyclase and PDE [7,8].

Since the embryonic stage of CaM research, CaM-dependent proteins have been continuously identified, and now include CaM kinases, phosphatases, metabolic enzymes, ion channels, ion pumps, transcription factors and many other proteins from yeast to humans [9]. Another remarkable feature of CaM is the diverse mechanisms underlying $Ca^{2+}$–CaM-dependent target regulation, and structural adaptations employed by CaM dependent upon the nature of the target protein, as previously reviewed [9,10]. This is extremely remarkable for such a small protein whose amino acid sequence is very highly conserved from yeast to humans (*i.e.* ranked

* Corresponding authors.
*E-mail addresses:* Peter.Stathopulos@schulich.uwo.ca (P.B. Stathopulos), mikura@uhnres.utoronto.ca (M. Ikura).

http://dx.doi.org/10.1016/j.bbrc.2015.01.106
0006-291X/

5th after histones H4 and H3, β-actin, and ubiquitin [11]). It is now well-appreciated that the keys for such 'multi-talented' function stem from the three-dimensional (3D) structure of CaM, as we will discuss in this review.

Over the past decades, there have been many excellent review articles and books which provide an overview of CaM research (*e.g.* Refs. [7,10,12–14]). In addition, an online 'Calmodulin Target Database' was established in 2000 (http://calcium.uhnres.utoronto.ca/ctdb.html; [15]), which has been widely used by the $Ca^{2+}$ signalling community. This database features sequence and structural analyses of CaM-binding motifs, such as those found in $Ca^{2+}$–CaM-dependent protein kinases, and provides a tool to identify CaM-binding sites within uncharacterized proteins based on previous knowledge available before 2000. However, as the CaM target interactome continues to grow, it is difficult to cover the continuously-expanding literature within databases, reviews or book chapters. In this article, we attempt to highlight several key findings about the CaM target interactome that highlight the multiple actions and recognition modes of CaM towards numerous targets, as well as the recent identification of disease-associated mutations of CaM.

The CaM superfamily represents a large group of $Ca^{2+}$ binding proteins that sense or buffer cytoplasmic $Ca^{2+}$, which includes troponin C, calbindins, S100s, recoverin, and many others [16–21]. However, until recently a major lack of understanding existed regarding how the cell senses $Ca^{2+}$ in intracellular organelles such as the endoplasmic reticulum (ER), a $Ca^{2+}$ store within eukaryotes. An exciting development in the $Ca^{2+}$ signalling field in the past decade was the discovery of a new $Ca^{2+}$ sensor protein tuned to the $Ca^{2+}$ levels of the ER. In immune cells such as T-cells and B-cells, it has been long recognized that $Ca^{2+}$ depletion from the ER initiates further $Ca^{2+}$ influx from outside of the cell, a phenomenon called 'store-operated calcium entry' (SOCE) first described by J.W. Putney Jr. in 1986 [22]. This phenomenon is critical for T-cell activation and now has been shown to exist in many other cell types including neurons and cardiac cells [23–27]. It is important to note that the ER $Ca^{2+}$ concentration is ~1000-fold higher ($10^{-4}$–$10^{-3}$ M) than that of the cytoplasm at most times within the cell; hence, CaM cannot function as a $Ca^{2+}$ sensor in the ER, as its $Ca^{2+}$ affinity is tuned to cytoplasmic $Ca^{2+}$ concentrations, which range from $10^{-7}$–$10^{-6}$ M [24].

It has long been a mystery how the cell detects ER $Ca^{2+}$ concentrations to precisely control $Ca^{2+}$ signalling events in response to various physiological cues. The answer to this question was resolved in 2005, with the discovery of stromal interaction molecule-1 (STIM1) as an ER-specific $Ca^{2+}$-dependent activator of plasma membrane (PM) $Ca^{2+}$ channels [28,29]. STIM1 can serve as a sensor of higher concentrations of $Ca^{2+}$, since it has a much lower affinity than CaM (see below). Remarkably, both STIM1 and CaM possess the EF-hand protein architecture, first discovered in parvalbumin by Kretsinger in 1973 [30–34]. Since the discovery of STIM1, numerous studies have been performed to understand the structure/function relationship of STIM1 as an ER-specific $Ca^{2+}$ sensor protein. The ER is not simply a $Ca^{2+}$ store in the cell, but also serves many other cellular functions including protein folding, stress response, protein transport, lipid biosynthesis, and post-translational modification [35,36], thus the identification of this ER $Ca^{2+}$-sensing protein provided unprecedented opportunities to investigate the molecular details of cross-talk between the $Ca^{2+}$-signalling apparatus in different compartments.

In this review, we discuss the structural and mechanistic characteristics of the key $Ca^{2+}$ sensing proteins, CaM and STIMs, as these proteins respond to $Ca^{2+}$ levels at opposite ends of the spectrum for CaM superfamily proteins. This comparison will highlight how the $Ca^{2+}$-sensing functions of CaM and STIMs have been specifically adapted by nature for roles in distinct cellular environments. Finally, we also discuss the recent findings from DNA sequencing studies on human patients, which revealed a number of disease-associated mutations in CaM and STIM proteins.

## 2. CaM structure and $Ca^{2+}$ binding

CaM is a 148-amino acid (a.a.) protein that is extraordinarily conserved to the extent that all vertebrates share an identical sequence, which is encoded by three genes in humans. CaM is also highly conserved in yeast and plants, which have multiple isoforms. The sequence comprises four EF-hands, each of which constitutes a $Ca^{2+}$-binding site. Each EF-hand contains a 12-a.a. acidic motif in the centre of a helix-loop-helix motif that coordinates a $Ca^{2+}$ ion *via* seven oxygen atoms. EF-hands are found in pairs in CaM and interact with each other through hydrophobic surfaces. The overall structure of CaM has been described as a dumbbell shape, comprised of N- and C-terminal independently folding domains or lobes, each containing a pair of EF-hands. The affinity for $Ca^{2+}$ of the C-terminal lobe is higher (equilibrium dissociation constant, $K_d$ ~0.4–10 μM) than that of the N-terminal domain ($K_d$ ~1.5–100 μM) in 100 mM KCl, pH 7.5, 25 °C [37]. Within each lobe the two EF hands bind two $Ca^{2+}$ ions cooperatively, whereas each lobe binds $Ca^{2+}$ independently of the other (in the absence of target peptide), although $Ca^{2+}$ affinity can be enhanced in the presence of a target protein [38].

In the first crystal structure of $Ca^{2+}$–CaM, the two lobes were connected through a central helix [30,34]; however, subsequent NMR structures of both $Ca^{2+}$-saturated [39–41] and apo-CaM [42–44] revealed that in solution this helix contains a flexible hinge region that confers mobility to the two lobes [43–45]. This linker enables the molecule to sample conformations in which the two lobes adopt different relative orientations and variable spacing, thus conferring structural 'plasticity', which is key for molecular recognition of the wide variety of CaM targets [12,46]. Each lobe of CaM undergoes a conformational change upon $Ca^{2+}$ binding that exposes hydrophobic methionine-rich target-protein binding sites [44] which interact with hydrophobic 'anchor' residues in target proteins. The flexibility of the methionine side chain confers yet another level of plasticity, enabling binding pockets of CaM to adapt to diverse target sequences and structures [12].

## 3. CaM-target complexes

CaM interacts with and regulates many proteins, including kinases [*e.g.* CaM kinase I (CaMKI), CaMKII, CaMKIV, CaMKK and MLCK], phosphatases [*e.g.* calcineurin (CaN)], membrane protein receptors [*e.g.* N-methyl-D-aspartate (NMDA) glutamate receptor, voltage-gated potassium ($K^+$), sodium ($Na^+$) and $Ca^{2+}$ channels, PM $Ca^{2+}$-adenosine triphosphatase (PMCA) pump, inositol 1,4,5 trisphosphate receptors ($IP_3R$) and ryanodine receptors (RyR)] as well as STIM and Orai proteins which mediate $Ca^{2+}$ release-activated $Ca^{2+}$ channel (CRAC) activity (see below). Extraordinarily, CaM can function as both a negative and positive feedback regulator for the myriad of $Ca^{2+}$-signalling toolkit proteins. For example, $Ca^{2+}$–CaM can bind to and inhibit RyR1 and RyR2 [47–51]. $IP_3Rs$ are also inhibited by CaM binding, although data have argued for both $Ca^{2+}$-dependent [52–54] and –independent [55,56] down-regulation [57]. On the other hand PMCA activity is upregulated by $Ca^{2+}$–CaM binding [58–62] as the PMCA auto-inhibition is relieved [63]. While the CaM interplay with $Ca^{2+}$ signalling toolkit components is complex, it is clear that the 'multi-talent' of CaM drives both positive and negative feedback regulation to precisely control $Ca^{2+}$ signals.

Some interactions between CaM and its targets are strictly dependent upon $Ca^{2+}$ for high affinity binding, while others are $Ca^{2+}$-independent, and some can interact with either $Ca^{2+}$-bound or $Ca^{2+}$-free (apo)-CaM [9]. Several channels contain separate $Ca^{2+}$-independent and -dependent binding sites, whereby the former sites are proposed to tether apo-CaM to the receptor such that it can rapidly access the latter sites in response to an influx of $Ca^{2+}$ [64]. CaM-binding domains (CBDs) are rich in hydrophobic and basic residues and often form amphipathic helical structures; however, their amino acid sequences are diverse. The structural details of target peptide recognition by CaM has been extensively studied, and an astounding number of CaM structures have been solved since the first structure in 1988 [30,34]. The protein data bank (PDB) currently contains more than 400 chains with >90% identity to vertebrate CaM, including structures of apo and metal-bound CaM, as well as CaM complexes with peptides, domains, and full-length target proteins, as well as small molecules and drugs. Here, we will present an overview of CaM-target complexes selected to highlight the diversity of binding modes discovered to date.

### 3.1. $Ca^{2+}$-dependent binding

$Ca^{2+}$-dependent interactions between CaM and a target protein usually involve two hydrophobic residues called 'anchors' (*e.g.* Trp, Phe, Leu, Val or Ile) on a helix within the target, each of which is bound by hydrophobic regions on one of the two lobes of CaM [65]. The spacing of these hydrophobic residues has been used to structurally classify target sequences. For example, in MLCK these anchor sites are separated by 12 residues [66,67] and are thus, described as a "1–14" motif [68]. Similar 1–14 motifs were subsequently identified in CaMKIV, CaN A, death-associated protein (DAP) kinase, and endothelial nitric oxide synthase (NOS). In CaMKII [69] as well as synapsins and heat-shock proteins, the hydrophobic anchor residues are separated by only 8 residues (*i.e.* "1–10" motif). In these 1–14 and 1–10 motif structures the N- and C-terminal anchor residues are bound to the C- and N-terminal lobes of CaM, respectively (*i.e.* antiparallel).

The anchor residues in CaMK kinase (CaMKK) are more widely spaced in sequence (*i.e.* "1–16" motif); however, this peptide adopts a helix and hairpin structure that effectively reduces the distance between these key residues, and strikingly, this peptide interacts with CaM in an orientation opposite to those discussed above (*i.e.* parallel) [70]. The peptide binding orientation appears to be determined primarily by electrostatic interactions. Most CBD peptides possess an N-terminal cluster of positively charged residues, which interact with an acidic patch in the C-lobe to stabilize the antiparallel orientation, whereas the CaMKK CBD has a cluster of positive residues in its C-terminal region, leading to parallel binding [70].

Recently, a crystal structure of $Ca^{2+}$–CaM in complex with a CBD from inositol 1,4,5-trisphosphate ($IP_3$) 3-kinase A, revealed another novel binding mode [71]. In this complex, the CBD peptide forms an α-helix followed by a hairpin-like loop containing the anchor residue that interacts with the C-lobe of CaM. The anchor residues in this CBD form a previously unknown 1–13 motif, and the relative position of the two CaM lobes resembles that of the CaM–CaMKK complex. Although the CaMKK 1–16 motif folds in a manner that brings the anchor residues together, recent structures of CaM complexes with RyR1 [72] and PMCA pump [63,73] CBDs reveal that CaM is able to bind longer, helical targets with "1–17" and "1–18" motifs, respectively, which requires disruption of most inter-lobe contacts as the CaM molecule extends. A structure of the entire regulatory domain of a plant PMCA in complex with two $Ca^{2+}$–CaM molecules bound to separate 1–14 motifs on a single long helix revealed a mechanism of two-stage regulation by $Ca^{2+}$ [74]. The pump is inactive in the absence of $Ca^{2+}$; however, binding of $Ca^{2+}$–CaM to the first site stimulates basal pump activity (*i.e.* stage 1) and occupation of both sites drives full activation of the pump (*i.e.* stage 2), as $Ca^{2+}$–CaM binding releases auto-inhibition.

In sharp contrast to these long helical motifs, the CaM binding site in myristoylated alanine-rich C kinase substrate (MARCKS) is largely intrinsically disordered with only a single turn of helix containing two hydrophobic residues separated by one lysine (*i.e.* "1–3" motif). The C-lobe of CaM engages one of these anchors in the classical hydrophobic pocket whereas the N-lobe remains in a closed conformation and interacts with the other anchor through a hydrophobic surface and associates closely with the C-lobe [75]. $Ca^{2+}$–CaM can also interact with two hydrophobic anchors that are not located in contiguous sequence. For example, in the interaction between CaM and plant glutamate decarboxylase (GAD), each lobe binds a separate monomer, thus activating enzymatic activity by inducing dimerization [76].

These studies of CaM in complex with isolated, minimal peptides have provided tremendous insight into the plasticity of CaM; however, they do not always reveal how the full-length protein is regulated by CaM and can sometimes yield structures that may not be physiologically relevant. For example, CaN has been crystallized as a domain-swapped hetero-tetramer with CaM in which each CaN peptide assumes an α-helical conformation and interacts with the N-lobe of one CaM molecule and the C-lobe of another [77]. By contrast, recent physicochemical characterization of this $Ca^{2+}$–CaM–CaN complex in solution [78] as well as a recent crystal structure [79] support a 1:1 complex formation which is consistent with numerous biochemical studies published thus far. Interestingly, no CaN residues are inserted into either hydrophobic pocket of CaM in this structure. Rather, side chains of I396/I400 and M406 of CaN are bound to the edges of C- and N-lobe hydrophobic pockets of CaM, respectively. Novel recognition modes of CaM are still being revealed.

### 3.2. IQ motifs and $Ca^{2+}$-independent binding

The apo form of CaM interacts with many proteins including 'unconventional' myosin [80], NOS [81], PDE [82], glycogen phosphorylase kinase [83], neuromodulin, neurogranin [84], IQGAPs [85], and numerous ion channels [9]. Many of these proteins contain an 'IQ motif' (IQXXXRGXXXR), many of which can interact with both apo-CaM and $Ca^{2+}$–CaM. Overall, less structural information is available for apo-CaM versus $Ca^{2+}$–CaM complexes with target peptides. The CaM-binding region of PDE forms a helix that interacts with both lobes of $Ca^{2+}$–CaM, whereas in the absence of $Ca^{2+}$, this peptide is less helical and binds with lower affinity only to the C-lobe of apo-CaM [82]. Two apo-CaM molecules bind tandem IQ motifs in myosin V with partially open C-lobes as well as closed N-lobes [86]. By contrast, apo-CaM binds to IQ motif peptides from the voltage-gated $Na_V1.2$ and 1.5 channels only through a semi-open C-lobe [87,88]. However, structures of $Ca^{2+}$–CaM bound to larger cytoplasmic C-terminal domains of $Na_V$ channels showed $Ca^{2+}$-dependent interactions between the N-lobe and an extended IQ helix [89]. L-type voltage-activated $Ca^{2+}$ channels ($Ca_V$) are regulated by CaM binding to an IQ motif and the 'preIQ' region in the C-terminal tail. $Ca^{2+}$–CaM in complex with the IQ domain of $Ca_V1.2$ wraps around the target helix to bind '1–10-motif' anchor residues with both lobes [90,91]. Interestingly, $Ca^{2+}$–CaM binds similar IQ domains from the voltage-activated $Ca_V2$ $Ca^{2+}$ channels in the opposite binding orientation [92]. Neuromodulin and neurogranin have IQ motifs that interact with apo-CaM, but dissociate in the presence of $Ca^{2+}$ [93]. These CBDs are intrinsically disordered in isolation, but become helical upon

binding CaM, similar to many $Ca^{2+}$–CaM-binding peptides. The structures of $Ca^{2+}$- and apo-CaM in complex with their diverse target motifs have been reviewed in extensive detail very recently [46].

## 4. Mechanisms of target protein activation

In 2000, Chin and Means proposed several general modes by which CaM regulates other proteins in the presence or absence of $Ca^{2+}$ [94]. 'Class A' proteins (*e.g.* phosphorylase kinase) associate irreversibly with CaM regardless of $Ca^{2+}$, thus CaM can be thought of a subunit. 'Class B' proteins (*e.g.* neuromodulin) bind CaM only in the absence of $Ca^{2+}$ and release activated $Ca^{2+}$–CaM upon $Ca^{2+}$ influx. 'Class C' and 'class D' proteins bind CaM weakly in the absence and strongly in the presence of $Ca^{2+}$, leading to activation (*e.g.* MLCK) or inhibition [*e.g.* $IP_3R$], respectively. Many CaM-regulated enzymes are constitutively regulated by auto-inhibitory domains which can be displaced through the binding of $Ca^{2+}$–CaM; however, other diverse mechanisms have been discovered including 'active site remodeling' and 'induced dimerization'.

### 4.1. CaM kinases and phosphatases

$Ca^{2+}$–CaM-dependent Ser/Thr protein kinases (*i.e.* CaMKs) [95] and phosphatases such as CaN [96–98] play critical roles in cellular $Ca^{2+}$ signalling, and have been the best characterized among CaM-binding proteins. Many X-ray and NMR structures have been reported for CBD peptides of CaMKs and phosphatases in complex with $Ca^{2+}$–CaM, including MLCK, CaMKI, CaMKII, CaMKK, DAP kinase (DAPK), and CaN [9]. CaMKs and CaN are activated by $Ca^{2+}$–CaM through analogous mechanisms [99]. These proteins each possess a catalytic (kinase or phosphatase) domain, an auto-inhibitory domain (AID), and a CaM-binding domain (CBD). Under basal $Ca^{2+}$ conditions, the AID occludes the substrate binding site of the catalytic domain. Upon elevation of the $Ca^{2+}$ level, $Ca^{2+}$–CaM binds to the CBD and displaces the adjacent AID from the substrate binding site, thus leading to the activation of the enzymes. It should be noted that phosphorylation at Ser/Thr residue(s) in the AID and/or CBD of CaM-dependent kinases is often involved in the regulation of the enzymatic activity (see below).

### 4.2. Structures of $Ca^{2+}$–CaM complexes with catalytic domains of CaMKs

How do the CBD recognition modes discussed above translate into physiologically relevant regulatory mechanisms? Crystal structures of $Ca^{2+}$–CaM in complex with larger CaMK constructs including the kinase domain, AID, and CBD have provided insight into this question. In the structure of $Ca^{2+}$–CaM–DAPK [100], CaM adopts an extended conformation compared to that in complex with the isolated CBD peptide. This extended $Ca^{2+}$–CaM conformation appears to be stabilized by direct interactions with the kinase domain, which account for a third of the total buried surface area (*i.e.* 656 $Å^2$ versus 1289 $Å^2$ for the CBD). However, $Ca^{2+}$–CaM bound to the DAPK kinase domain occludes the substrate binding site, suggesting that full kinase activity may involve a conformational change towards the more compact $Ca^{2+}$–CaM conformation observed in complex with the CBD peptide.

The activity of CaMKII is regulated not only by $Ca^{2+}$–CaM, but also by auto-phosphorylation of Thr residues in the AID (*i.e.* Thr286) and CBD (*i.e.* Thr305/Thr306). The auto-phosphorylated form acquires $Ca^{2+}$-independence, referred to as autonomy [101,102], which prolongs the lifetime of the active state of CaMKII and plays a role in long-term potentiation and memory [103]. Inter-subunit auto-phosphorylation of CaMKII is mediated by a C-terminal oligomerization domain. As observed for other CaMKs, at basal $Ca^{2+}$ levels the substrate binding site of the kinase domain is occluded by the AID, which is displaced by $Ca^{2+}$–CaM binding when the $Ca^{2+}$ level is elevated. Subsequently, Thr286 auto-phosphorylation leads to $Ca^{2+}$–CaM-independent CaMKII activation, although maximal kinase activity still requires $Ca^{2+}$–CaM [104]. Phosphorylation of Thr286 decreases the $Ca^{2+}$–CaM dissociation rate by 10,000-fold, which is referred to as $Ca^{2+}$–CaM-trapping [105,106]. A decrease in the $Ca^{2+}$ concentration leads to dissociation of CaM, followed by auto-phosphorylation of Thr305/Thr306 in the CBD, which prevents rebinding of CaM, even in the presence of $Ca^{2+}$.

Insight into the structural mechanisms of CaMKII activation has been gained through a number of crystal structures and physicochemical characterizations [107]. The crystal structure of the auto-inhibited form of an intact holoenzyme elucidated the structural basis for inter-subunit interaction and assembly of a dodecamer (Fig. 1) [108]. However, two distinct crystal structures were reported for CaMKII truncation mutants lacking the oligomerization domain. The AID assumes an α-helical conformation with Thr286 buried in the substrate binding site in both structures; however, one structure forms a dimer mediated by a coiled-coil in the CBD [109], whereas the other structure is monomeric with an unstructured CBD and Thr307 (CaMKIIδ numbering) inserted into the catalytic site [110]. In the structure of the $Ca^{2+}$–CaM-bound form of truncated CaMKIIδ lacking the oligomerization domain (Fig. 2) [110], the CBD forms an α-helix while the AID including the auto-phosphorylation site Thr287 (CaMKIIδ numbering) adopts an extended conformation. The extended AID is recognized by the catalytic subunit of the adjacent CaMKII subunit, enabling inter-molecular auto-phosphorylation of Thr287; however, phosphorylation of Thr307 is prevented by the bound $Ca^{2+}$–CaM. When CaM dissociates upon reduced $Ca^{2+}$ levels, Thr307 is subject to *cis*-autophosphorylation which prevents $Ca^{2+}$–CaM binding and thus results in $Ca^{2+}$-insensitivity of CaMKII [111].

### 4.3. Activation mechanisms of other CaM targets

CaN, the best-studied Ser/Thr phosphatase that is regulated by $Ca^{2+}$–CaM, is activated by CaM through displacement of a C-terminal auto-inhibitory domain. CaN activates nuclear factor of activated T-cells (NFAT), which can be blocked by the immunosuppressive drug cyclosporine. A number of exciting developments have elucidated the action of cyclosporine in CaN inhibition [112,113] as well as the substrate-recognition and regulatory mechanisms of CaN involving the $Ca^{2+}$ binding subunit (CaN B) [114]. However, no structure has been reported for the CaN catalytic subunit (CaN A), including CBD in complex with $Ca^{2+}$–CaM.

A series of crystal structures of $Ca^{2+}$–CaM in complex with the flavin mononucleotide domain of inducible NOS suggest that CaM binds the 1–14 helical motif in the same manner as it binds the isolated peptide. This CBD blocks the flow of electrons from flavin to heme, but is displaced by CaM binding to relieve this auto-inhibition [115].

### 4.4. Target regulation by extended conformations of CaM

Some CaM target proteins are activated by allosteric mechanisms. *Bacillus anthracis* produces a toxin called edema factor (EDF), an adenylyl cyclase that is activated by CaM only when secreted into a eukaryotic host cell. The two lobes of CaM bind non-contiguous sites in EDF, and induce 'active site remodeling' [116] whereby the $Ca^{2+}$-bound C-terminal lobe and $Ca^{2+}$-free N-lobe stabilize the active conformation of EDF. CaM also modulates the

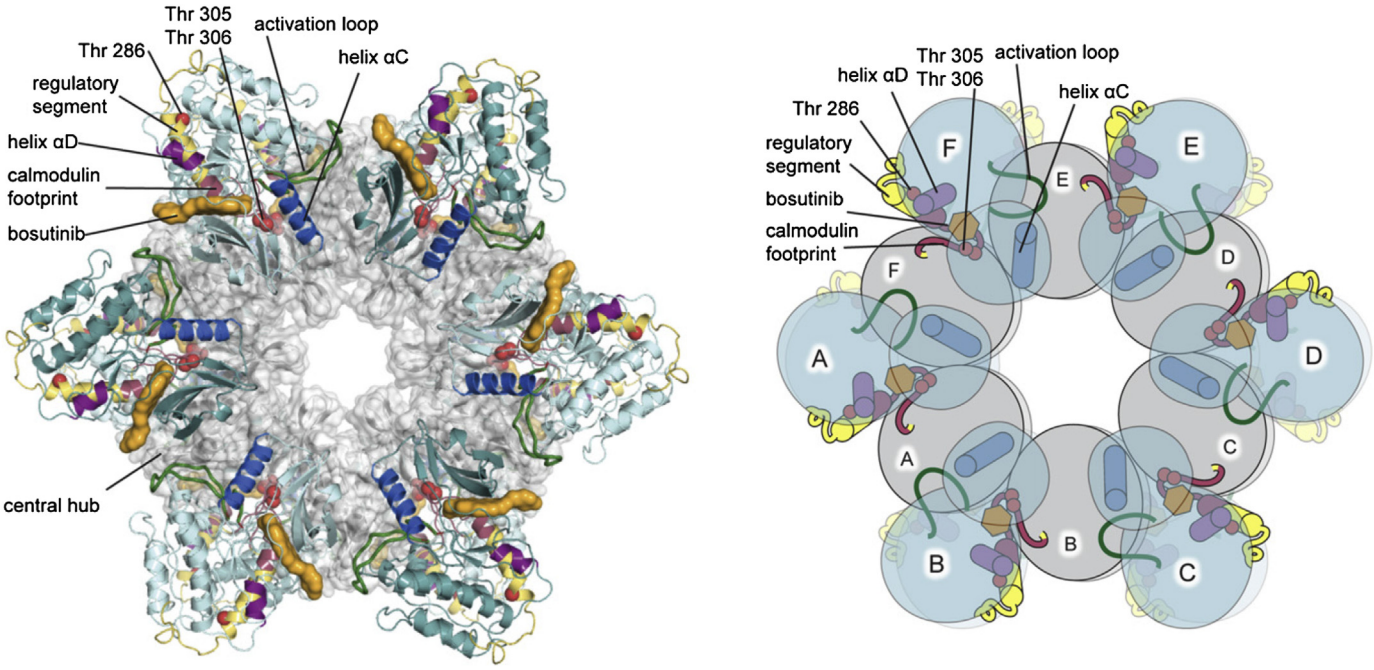


**Fig. 1.** Dodecameric assembly of CaMKII. Two separate hexameric rings of kinase make up the CaMKII dodecamer. Each kinase domain (cyan) is packed between two hub domain subunits (grey), with the active sites pointed toward the centre of the hub. The activation loop is shown in green, helix αC in blue, helix αD in purple, regulatory segment in yellow, CaM footprint in red and the phosphorylation sites (Thr286, Thr305, Thr306) as red spheres. The figure is reproduced from Ref. [108] with permission from Elsevier.

conductance of many ion channels, often by inducing dimerization. Small conductance $Ca^{2+}$-activated potassium (SK) channels are opened by $Ca^{2+}$—CaM binding to a C-terminal region. The 96-residue CaM-binding region of SK2a lacks canonical CaM-binding motifs and forms two interacting helices connected by a loop [117]. Two SK peptides form an antiparallel dimer with a three-helix bundle at each end, and CaM interacts in a 2:2 complex in which the N- and C-lobes bind different subunits. Each C-lobe binds

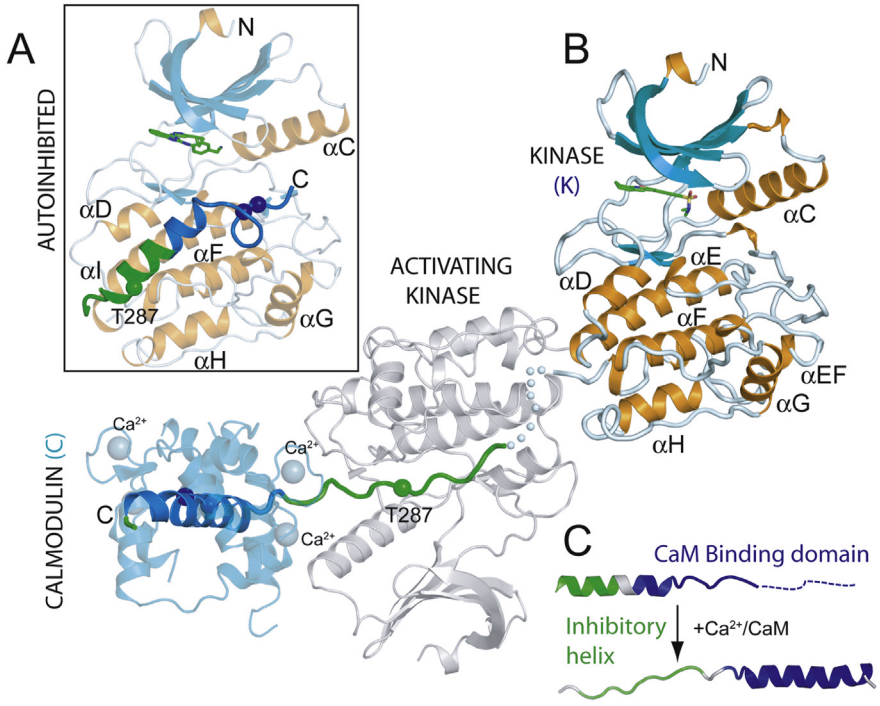


**Fig. 2.** Structure of the CaMKIIδ/$Ca^{2+}$—CaM complex. (A) Auto-inhibited CaMKIIδ kinase. The Thr287, Thr306, Thr307 phosphorylation sites are shown as spheres. The CaM binding site is coloured blue and the auto-inhibitory region is coloured green. (B) The $Ca^{2+}$—CaM/CaMKIIδ complex structure. CaM is coloured cyan, while the CaM binding domain is blue. The Thr287 phosphorylation site is indicated (green sphere). (C) Structural transformation of the auto-regulatory domain upon $Ca^{2+}$—CaM binding. The inhibitory helix is shown in green while the $Ca^{2+}$—CaM binding domain is shown in blue. $Ca^{2+}$—CaM binding causes a loss in structure in the inhibitory helix concomitant with a gain in structure in the CaM binding domain. The figure is reproduced from Ref. [110] with permission according to the Creative Commons Attribution (CC BY) license.

one helix in a $Ca^{2+}$-independent manner whereas each N-lobe binds a pair of helices in a $Ca^{2+}$-dependent manner. SK2a also interacts with apo-CaM in a manner that involves only the C-lobe [118]. CaM binding stabilizes SK2a dimerization in response to $Ca^{2+}$, which leads to channel opening. The splice variant SK2b also crystallized with CaM in a 2:2 complex, but adopts a different configuration with no direct interactions between the SK2b peptides and both lobes $Ca^{2+}$ bound [119].

CaM can also induce dimerization of voltage-gated $Ca^{2+}$ channels. The 'pre-IQ' and IQ motifs of the L-type $Ca_V1.2$ channel crystallized as a dimer in complex with four $Ca^{2+}$–CaM molecules [120,121]. The pre-IQ regions formed a long coiled-coil bridged by two $Ca^{2+}$–CaM, while two additional $Ca^{2+}$–CaM were bound to the IQ motifs; however, the physiological relevance of dimerization is uncertain. L-type $Ca^{2+}$ channels also interact with apo-CaM which has been thought to serve primarily to localize CaM to the channel such that it can rapidly inhibit channel opening in response to $Ca^{2+}$ influx; however, a recent model holds that apo-CaM directly stimulates L-type $Ca^{2+}$ channel opening, which is reversed by $Ca^{2+}$ influx [122].

## 5. Disease-associated CaM mutations

Until very recently, no disease-associated mutations had been reported in CaM. Considering the extraordinary conservation of CaM, the apparent absence of mutations in the three genes encoding CaM (*CALM1*, *CALM2*, *CALM3* located on chromosome 14q24-q31, 2p21.1-p21.3, and 19q13.2-q13.3, respectively [123]) seemed consistent with a general notion that any mutations of CaM would have such profound effects that they would likely be lethal. However, over the last three years, at least ten CaM mutations have been identified in a small number of patients with cardiac arrhythmias. The main phenotype associated with these mutations is remarkably specific to the heart and sometimes accompanied by neuro-developmental delays. Although the number of affected individuals identified remains small, the emerging trend suggests that there may be multiple, somewhat overlapping classes of mutations associated with distinct types of arrhythmias, which act through different mechanisms.

In 2012, Nyegard et al. reported two missense mutations in the *CALM1* gene identified in patients with catecholaminergic polymorphic ventricular tachycardia (CPVT) [124], an arrhythmia associated with sudden cardiac arrest following exercise or emotion (*i.e.* adrenergic activation). CPVT is thought to be a significant cause of unexplained sudden cardiac deaths amongst young people, and most cases of dominantly inherited CPVT are caused by mutations in RyR2 [125]. One of the two CaM mutations (N53I) was dominantly inherited in a large family with severe CPVT, whereas the second (N97S) arose *de novo*. N53 is located on a solvent-exposed surface of the N-lobe, whereas N97 is part of the $Ca^{2+}$-binding EF-hand in the C-lobe [124] (Fig. 3).

The following year, additional missense mutations in *CALM1* (D129G and F141L) and *CALM2* (D95V) were reported in infants exhibiting long QT syndrome (LQTS) with recurrent cardiac arrest [126]. LQTS is often associated with loss-of-function $K^+$ channel mutations or gain-of-function mutations of $Na^+$ or $Ca^{2+}$ channels [127,128], however genetic analyses of patients with unexplained LQTS identified *CALM2* missense mutations [129], including N97S (analogous to the CPVT *CALM1* mutation, suggesting possible isoform-specific phenotypes) and N97I [129]. This study also identified *CALM2* D131E and Q135P in children exhibiting clinical features of both LQTS and CPVT, as well as *CALM1* D133H [129]. Another LQTS-associated mutation was recently identified in *CALM3*, analogous to the *CALM1* D129G mutant [130]. These LQTS-associated variants were determined to be *de novo* mutations, and affect the EF-hands in the C-lobe, thus reducing $Ca^{2+}$ affinity 5–50-fold [126,129,131]. Interestingly, the N97S mutation, which was seen in CPVT and LQTS patients had a modest effect on $Ca^{2+}$ binding (<2–3 fold) [124,131], whereas the N-lobe CPVT-associated mutation N53I had no significant effect [124,131].

Unlike LQTS and CPVT, idiopathic ventricular fibrillation (IVF) can result in sudden cardiac death in the absence of identifiable electrocardiogram features. Recently, a *CALM1* mutation encoding F89L was associated with IVF [132]. F89 is not in an EF-hand, but is found in the interdomain linker, where it interacts with some CaM target peptides. Human CaM F89L has not been functionally characterized; however, in yeast a F89A mutation disrupts binding to CaMK, but not CaN [133], suggesting this IVF-associated mutation may deregulate a specific subset of CaM target proteins.

Considering the broad range of functions served by CaM, the cardiac-specific phenotype associated with CaM mutation is somewhat surprising. CaM regulates cardiac contractility through multiple channels, including L-type voltage gated $Ca^{2+}$ channels, $K^+$ channels, $Na^+$ channels, and RyR2, which mediates $Ca^{2+}$-induced $Ca^{2+}$ release (CICR), and many of the cardiac ion channels are modulated by CaM targets including adenyl cyclases, PDE and CaMKII [134]. It is also surprising that these CaM mutations act in a dominant fashion, despite the presence of three *CALM* genes. All three *CALM* genes are expressed in the heart [126,134]; thus, a single mutant allele induces a phenotype, even in the presence of five normal alleles.

CPVT is most commonly caused by gain-of-function RyR2 mutations [125], or mutations affecting RyR2-binding proteins (*i.e.* calsequestrin-2 and triadin) [135], which lead to spontaneous opening and $Ca^{2+}$ waves that trigger membrane depolarization. CaM binding to RyR2 decreases its open probability, and RyR2 mutations that disrupt CaM binding are associated with spontaneous $Ca^{2+}$ release [136]. CaM N97S, but not N53I, exhibited reduced binding to the RyR2 CBD peptide at low $Ca^{2+}$ concentration (100 nM); however, neither mutation affected binding at $\geq$1 mM $Ca^{2+}$ [124]. Nyegaard et al. proposed that the impaired binding of the N97S CaM mutation causes deregulation of RyR2 [124]; however, it is not clear how a mutant with impaired RyR2 binding could exert a dominant effect over wild-type CaM.

Hwang et al. examined how CaM mutations affect binding to full-length RyR2 and $Ca^{2+}$ waves in cardiomyocytes [131]. The CPVT-associated mutations N53I and N97S significantly increased the frequency and decreased the amplitude of $Ca^{2+}$ waves, similar to RyR2 mutations, whereas LQTS-associated mutations did not affect (F141L and D95V) or slightly decreased $Ca^{2+}$ wave frequency (D129G) [131]. In contrast to the isolated RyR2 peptide, the CPVT mutants exhibited higher affinity than wild-type CaM for full-length RyR2 at 30 nM $Ca^{2+}$; however, despite tight binding, the N97S mutant failed to inhibit RyR2 conductivity and N53I surprisingly increased the RyR2 open probability [131]. Remarkably, the CPVT-associated mutants were capable of increasing $Ca^{2+}$ wave frequency even in the presence of 8-fold excess wild-type CaM, consistent with their higher affinity for full-length RyR2 [131]. In contrast, the LQTS-associated CaM mutant D95V inhibited RyR2 normally, while D129G and F141L reduced RyR2 binding [131]. In summary, CPVT-associated CaM mutations maintain binding to RyR2, but fail to inhibit the channel, whereas LQTS-associated mutants either bind and regulate RyR2 normally or do not compete with wild-type CaM and therefore do not affect RyR2 function. The structural basis for the higher affinity of the CPVT mutants to full-length RyR2 despite reduced binding to the CBD peptide, and the mechanism underlying their failure to inhibit RyR2 remain to be elucidated. The regulation of RyR2 by CaM is not fully understood; both apo-CaM and $Ca^{2+}$–CaM interact with RyR2, which contains more than one binding site [72,137–140].

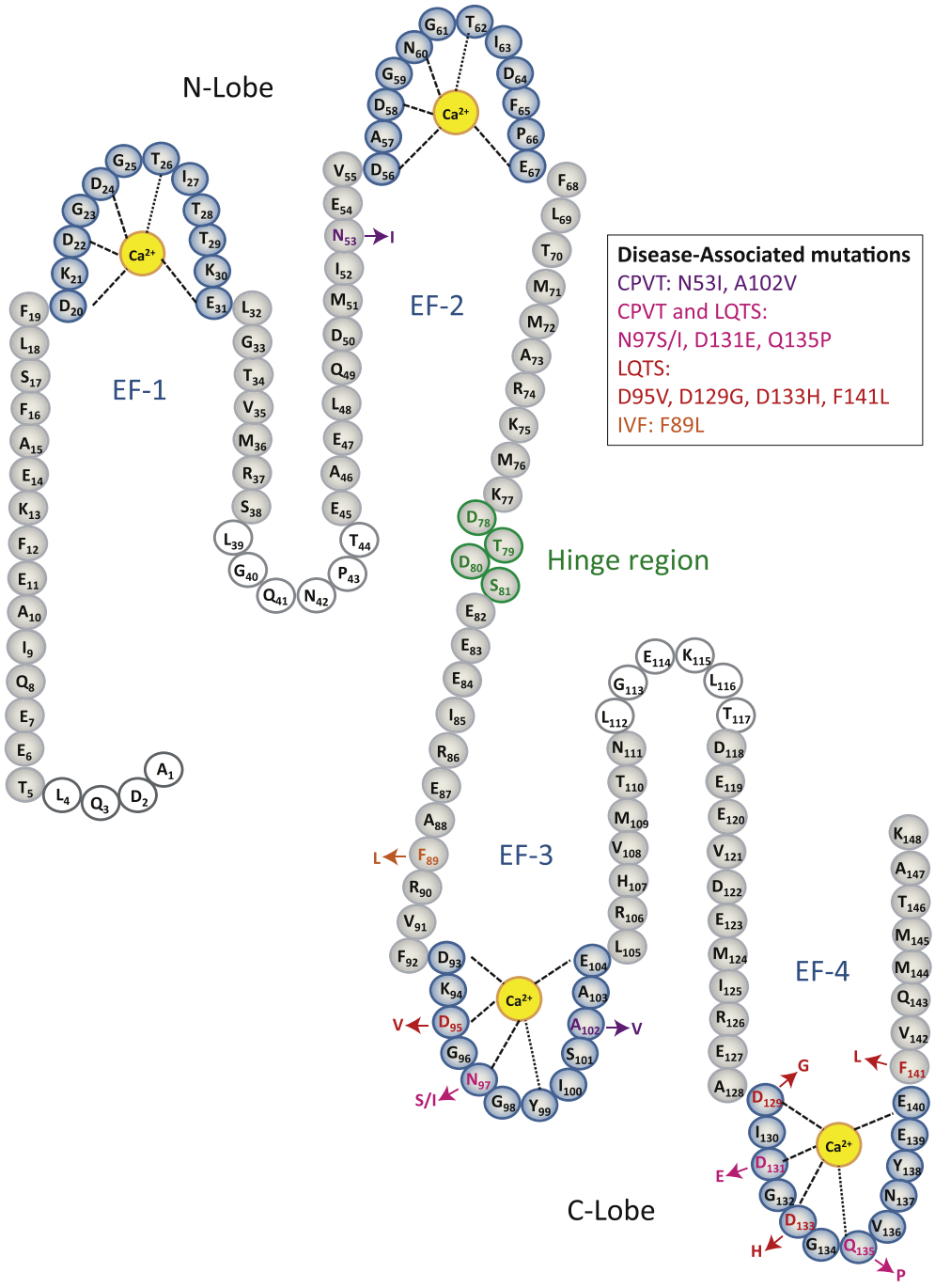


**Fig. 3.** Structural features and sites of disease-associated mutations in CaM. Schematic representation of the CaM sequence with the four EF hands indicated and $Ca^{2+}$-coordinating loops in blue and helical residues in grey. Coordination of $Ca^{2+}$ ions through side-chain and backbone oxygens are indicated by dashed and dotted lines, respectively. The flexible hinge region of the inter-lobe linker is shown in green. Mutations associated with catecholaminergic polymorphic ventricular tachycardia (CPVT, purple), long QT syndrome (LQTS, red), features of both CPVT and LQTS (magenta), and idiopathic ventricular fibrillation (IVF, orange) reported in Refs. [124,126,129,131,132,144] are indicated.

Although the LQTS-associated CaM mutations do not affect the function of RyR2, Limpitikul et al. demonstrated that expression of D95V, D129G or F141L in ventricular myocytes increases $Ca^{2+}$ transients and suppresses the $Ca^{2+}$–CaM-dependent inactivation of L-type $Ca^{2+}$ channels, thus increasing $Ca^{2+}$ influx, even in the presence of excess wild-type CaM [141]. In contrast, the CPVT-associated mutants had little or no effect on the function of L-type $Ca^{2+}$ channels. $Ca^{2+}$-dependent regulation of L-type $Ca^{2+}$ channels by $Ca^{2+}$–CaM requires the pre-association of apo-CaM [64,142]. Thus, LQTS-associated CaM mutants with impaired $Ca^{2+}$ binding may compete with wild-type CaM for the apo-CaM binding site, but fail to inactivate the channel in response to a $Ca^{2+}$ signal. The dominant phenotype is also consistent with the recent model that apo-CaM serves as a direct activator of voltage gated $Ca^{2+}$ channels that is terminated upon $Ca^{2+}$ influx [122]. LQTS mutants with impaired $Ca^{2+}$ binding may continue to activate the channel in the presence of $Ca^{2+}$ and might, thereby, be viewed as gain-of-function rather than loss-of-function mutants, consistent with

their dominant effect. Preassociation of apo-CaM is also essential for regulation of some voltage gated $Na^+$ and $K^+$ channels, suggesting that LQTS CaM mutants may affect additional channels through analogous mechanisms, although Yin et al. found that they have little effect on L-type $Na^+$ channels [143].

### 5.1. CaM in cancer

Very few non-synonymous variants of CaM genes have been observed in the Exon Sequencing Project (*CALM1* I9T and V142L, and *CALM3* A102T). No phenotypic information is available for the individuals with these variants, although A102V has been associated with CPVT [144]. In contrast, many somatic mutations of CaM genes have been observed in tumours by cancer genome sequencing efforts. The COSMIC database currently lists the following missense mutations (*CALM1*: K30E, M36T, G59S, P66L, L69F, M72I, R74I, R106C/H, N137S; *CALM2*: D2A, F12L, G25E, I27V, S38Y, G40E, Q41H, G61D, D78E, E84K, R86T, K94E, G96A, R106C, E114K, G132A, Y138C; *CALM3*: Q8H, D22E, T29S, E104Q, M144V), and two nonsense mutations predicted to encode truncated CaM variants lacking a functional C-lobe (*CALM1* E67*, R90*). We are not aware of any data investigating whether these *CALM* mutations contribute to oncogenic signalling or are simply 'passenger' mutations resulting from the DNA repair defects that accumulate in cancer cells.

In recent years, CaM has been implicated in oncogenic signalling through an interaction with the oncogenic protein Kirsten rat sarcoma (KRAS)4B. *KRAS* is one of the most frequently mutated genes in human cancer, with activating mutations found in 22% of all tumours, including 61% of pancreas, 33% of colon and 17% of lung cancers [145]. KRAS4B consists of a guanosine triphosphatase (GTPase) domain and a flexible, polybasic, farnesylated, C-terminal tail that anchors it to the PM. The KRAS4B–CaM interaction has been reported to be $Ca^{2+}$- and GTP-dependent, and to involve the farnesyl group, the lysine-rich region and the GTPase domain [146–148], and is thought to reduce KRAS4B affinity for the PM [147,149,150]. KRAS4B depends upon basic residues in the tail for its dynamic membrane association [151,152], and protein kinase C (PKC) phosphorylation of a Ser in this region reduces the positive charge and leads to its redistribution to endomembranes [153] where it induces autophagy [154]. CaM is antagonistic with PKC, as bound CaM protects the site from PKC phosphorylation, and conversely, phosphorylation disrupts CaM binding [146,147,150,155]. Structural details of this interaction are lacking; however, the KRAS4B tail lacks hydrophobic anchor residues and it has been proposed that CaM may sequester the farnesyl moiety of KRAS4B in a manner reminiscent of its interaction with the myristoyl groups of MARCKS and cortical cytoskeletal associated protein (CAP-23)/neuronal axonal myristoylated membrane protein (NAP-22) [156,157]. A better understanding of the interplay between KRAS4B, PKC and CaM may reveal therapeutic opportunities for modulating the balance of oncogenic versus anti-proliferative functions of KRAS4B.

## 6. Stromal interaction molecule $Ca^{2+}$ sensors

STIM1 and STIM2 are the $Ca^{2+}$ sensory protein machinery specialized for function in the ER [28,29,158]. Together with PM-resident $Ca^{2+}$ Orai channels [159–162], these proteins constitute the minimal complex required to establish SOCE [163,164], which mediates a plethora of physiological processes such as transcription, apoptosis, the immune response, thrombosis as well as pathophysiological processes such as carcinogenesis, cardiac hypertrophy and immunodeficiency-related disease, to name a few. While STIM1 is ubiquitously expressed in most tissues and is involved in regulation of SOCE, STIM2 appears to be more concentrated in neuronal tissues and plays a major role in maintaining basal $Ca^{2+}$ levels in the cytoplasm and ER [165,166]. STIMs are single-pass transmembrane (TM) proteins of ~77 kDa. STIMs possess a highly conserved N-terminal EF-hand domain, consisting of a canonical $Ca^{2+}$ binding EF-hand (cEF) motif, a non-canonical EF-hand (ncEF) motif and a sterile α motif (SAM) domain located within the ER lumen, whereas the C-terminal cytoplasm-oriented region contains three conserved coiled-coil domains (CC1, CC2, CC3) in tandem, followed by Ser/Pro-rich and Lys-rich regions (Fig. 4A). While the luminal EF-hand together with the SAM domains (EF-SAM) sense changes in $Ca^{2+}$ levels [167,168] (see below), the cytoplasmic domains organize the assembly and gating of PM Orai1 subunits into open CRAC channels [169–171].

## 7. $Ca^{2+}$ binding and STIM1 EF-SAM structure

STIM1 was first identified as a $Ca^{2+}$ sensor in the ER involved in SOCE by two independent RNA interference (RNAi) studies in 2005 [28,29]. Compared to the archetypal cytoplasmic $Ca^{2+}$ sensor CaM (see CaM section of this review), the affinity of $Ca^{2+}$ to the STIM1 and STIM2 EF-SAM domains is relatively low ($K_d$ for CaM ~μM versus ~sub-mM for STIM EF-SAM domains) [37,168,172,173]. This dramatic difference in $Ca^{2+}$ affinity between CaMs and STIMs exist despite a high conservation of the loop residues that coordinate $Ca^{2+}$ within the first EF-hand (*i.e.* STIM cEF) (Fig. 4B). EF-hand loop residue positions 1, 3, 5, 7 and 9 provide monodentate $Ca^{2+}$ ligands while residue 12 contributes bidentate ligands to create a pentagonal bipyrimidal geometry in canonical EF-hand $Ca^{2+}$ coordination [14]. Residues 1, 3 and 5 invariantly contribute side chain oxygen ligands, residue 7 contributes a backbone carbonyl oxygen ligand positioned by an invariant Gly at position 6 that facilitates a sharp turn in the loop; moreover, residue 9 can provide a side chain oxygen or $H_2O$ oxygen while residue 12 contributes two oxygen side chain atoms to the coordination [13,14,18]. The reason for the weaker $Ca^{2+}$ affinity in the EF-SAM domains may be related to the non-canonical loop sequence (ncEF) of the second EF-hand motif that makes up the EF-hand pair in STIMs. The ncEFs of the human STIMs do not possess the necessary acidic residues in position 1 and 3, and the vital Gly at position 6 is replaced by Lys in STIM1 and STIM2; moreover, the position 12 residue of the loop is occupied by a shorter Asp side chain which may not be ideal for $Ca^{2+}$ coordination (Fig. 4B). As predicted from the sequence of the EF-hand loops, STIM EF-SAM domains bind a single $Ca^{2+}$ ion based on NMR titration, native-like mass spectrometry and radioisotope measurements [33,168,172,173]. The ~1000-fold weaker STIM EF-SAM $Ca^{2+}$ affinity compared to CaM make these molecules ideal sensors for ~1000-fold higher $Ca^{2+}$ levels of the ER lumen, whereas the higher $Ca^{2+}$ affinity of CaM is tailored to the much lower $Ca^{2+}$ levels in the cytoplasm [24,37].

NMR based solution structural studies of the STIM1 EF-SAM domain revealed that it forms a single compact structure comprised of 10 α-helices and two short β-strands in the $Ca^{2+}$-loaded holo state [33]. The cEF (α1-β1-α2) is paired with the ncEF (α3-β2-α4) through backbone H-bonding between the β1 and β2 strands (Fig. 5A). However, the ncEF does not bind $Ca^{2+}$. The EF-hand domains of STIMs are linked in sequence space by a short helix (α5) where the SAM domain folds in a 5-helix bundle (α6–α10); however, the SAM domain packs tightly into a hydrophobic cleft formed by the EF-hand pair through C-terminal anchor residues (*i.e.* Leu195 and Leu199), forming a single compact entity (Fig. 5A). The two STIM anchor residues form intramolecular interactions with the hydrophobic cleft of the EF-hand domain, reminiscent of the mode of intermolecular target interactions by

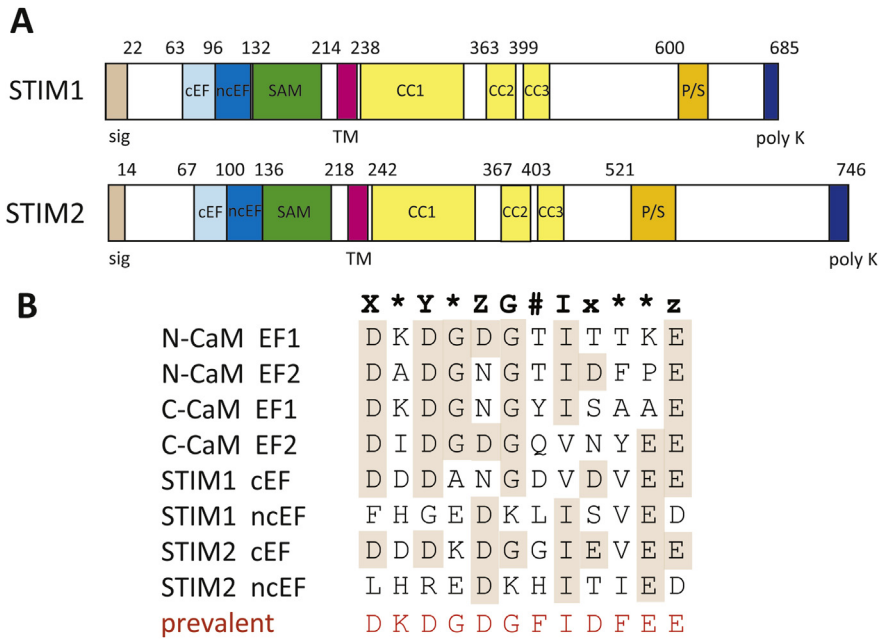


**Fig. 4.** Domain architecture of STIMs and $Ca^{2+}$ binding loop sequence alignment. (A) Domain architecture of human STIM1 and STIM2. Abbreviation for the domains are as follows: sig, signalling peptide sequence; cEF, canonical EF-hand; ncEF, non-canonical EF-hand; SAM, sterile α-motif; TM, transmembrane region; CC1-CC3, coiled-coil region 1–3; P/S, Pro and Ser rich region; poly K, Lys rich region. (B) Sequence alignment of the EF-hand $Ca^{2+}$ binding loops for human CaM and STIMs. The position code of the residues is shown at the top (bold). X, Y, Z, # and x contribute monodentate and z contributes bidentate ligands in the $Ca^{2+}$ coordination. G and I are invariant. The most prevalent residues at each position are shown at the bottom (red) [219]. Conserved residues within the aligned loops are shaded pink.

CaM where target anchor residues are directed into the CaM hydrophobic EF-hand pocket [66,67].

Remarkably, there are currently no structural homologues of STIM EF-SAM domains within the PDB despite the frequent occurrence of EF-hand and SAM domains within the proteome; nevertheless, a DALI search [174] for structural homologues of the STIM1 EF-hand domain reveals the closest homologue is the $Ca^{2+}$-loaded C-terminal bovine CaM domain [*i.e.* backbone atom root mean square deviation (rmsd) = 3.2 Å] (Fig. 5B). It is clear from a structural alignment of the STIM1 EF-hand domain with C-terminal CaM is that both domains adopt an 'open' conformation, defined by interhelical angles greater than approximately 70°, a hallmark of many $Ca^{2+}$ loaded EF-hands that results in exposure of hydrophobic residues for target binding. The STIM1 EF-SAM cEF and ncEF interhelical angles are 80.0° and 96.7°, respectively, compared to the C-terminal CaM EF-hands which are 81.4° and 107.7° (Fig. 5B). The structural similarity of the $Ca^{2+}$-loaded EF-hand angles and the anchor residues provided by target peptides suggest that STIM binds to its target (*i.e.* the SAM domain) through a strikingly similar mechanism as the classical CaM mechanism of target binding, despite low overall sequence similarity and orders-of-magnitude differences in $Ca^{2+}$ binding affinity. The STIM1 SAM domain most closely resembles the SAM domain of the EphB2 receptor (*i.e.* backbone rmsd = 2.1 Å) suggested to be involved in oligomerization of the protein [175]. SAM domains are known protein interaction domains [176], and the presence of SAM in the luminal domain of STIMs is not surprising given the significance of oligomerization to the SOCE activation process (see below).

## 8. STIM1 $Ca^{2+}$-dependent luminal activation process

While the separately considered EF-hand domain and SAM domain adopt tertiary folds similar to other known domains, the EF-hand:SAM intramolecular interaction is more unique. In the presence of $Ca^{2+}$, extensive contacts between the hydrophobic cleft made by the EF-hand pair and the protruded hydrophobic residues (anchor residues) of the SAM domain maintain EF-SAM in close association. The significance of this interaction is underscored by the facts that each subdomain is destabilized significantly in the absence of the other or by mutations that disrupt the critical interface [33,168,177]. When $Ca^{2+}$ is depleted from the ER lumen, a $Ca^{2+}$ depletion-dependent EF-SAM destabilization coupled with oligomerization occurs [168,173]. The importance of EF-SAM oligomerization in the context of full-length physiological function of STIM1 was demonstrated by a study of live cells expressing STIM1 variants in which the luminal domain was replaced by FKBP12 or FK506 domains [167], which can be pharmacologically induced to oligomerize by rapamycin. This chimeric STIM1 did not exhibit ER luminal $Ca^{2+}$ sensitivity; however, rapamycin-induced oligomerization activated SOCE [167]. Moreover, STIM1 truncated after the TM region displays little intermolecular FRET at resting ER $Ca^{2+}$, but shows high intermolecular FRET after ER $Ca^{2+}$ depletion, indicating that the self-association of the N-terminal region is $Ca^{2+}$-depletion dependent [178]. Overall, these data unequivocally demonstrate that EF-SAM oligomerization is an important initiation step in STIM1 and SOCE activation.

*In vitro* studies have provided further details on the mechanism of EF-SAM oligomerization. Multi angle light scattering (MALS), chemical cross-linking and analytical ultracentrifugation show that STIM1 EF-SAM tends to self-associate to form a dimer as a major species upon $Ca^{2+}$ chelation at low temperature (4 °C) [168,179]. The data also indicate the presence of higher oligomer species and polymorphic forms depending on temperature and protein concentration [168,172]. At present, the physiological significance of the higher-order EF-SAM oligomers is not clear; however, it has been demonstrated that simple disulfide tethering of the N-terminal CC1 region, corresponding to the portion of STIM1 closest to the cytoplasmic side of the ER membrane, can increase the activity of SOCE, suggesting an important role for dimerization of EF-SAM in the activation process [180].

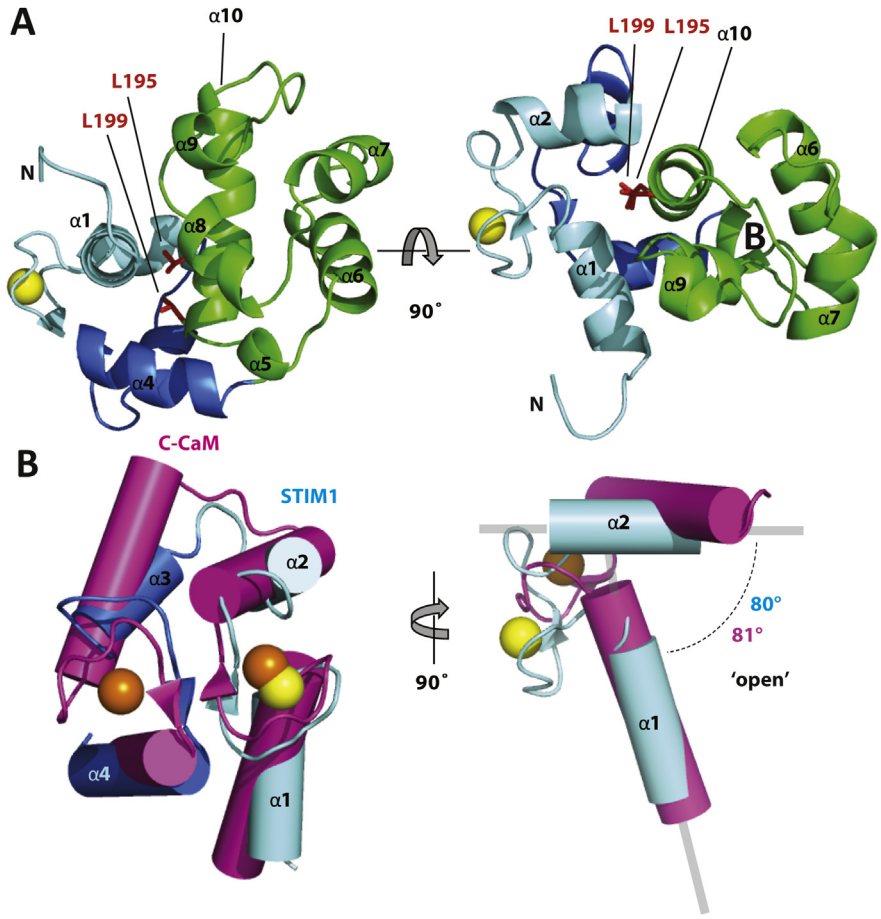


**Fig. 5.** STIM1 EF-SAM structural comparison with CaM. (A) Solution NMR structure of the STIM1 EF-SAM domain. The canonical EF-hand (cEF), non-canonical EF-hand (ncEF) and SAM domain are coloured cyan, blue and green, respectively. The C-terminal anchor residues of SAM domain are shown as red sticks. The $Ca^{2+}$ ion is shown as a yellow sphere. The images were rendered in PyMOL using 2K60.pdb. (B) Structural alignment of STIM1 and C-terminal CaM domain (C-CaM) EF-hand domains. The STIM1 cEF and ncEF are shown in cyan and blue respectively, structurally aligned with the two EF-hand motifs making up bovine C-CaM (magenta, left). At right, cEF of STIM1 is superimposed with the first EF-hand motif in C-CaM showing a remarkably similar interhelical angle indicative of the 'open' EF-hand conformation. The $Ca^{2+}$ ions of STIM1 and CaM are shown as yellow and orange spheres, respectively. The images were rendered in PyMOL using 2K60.pdb and 1PRW.pdb.

Upon $Ca^{2+}$ dissociation from EF-SAM, the far-UV circular dichroism (CD) spectra shows reduction in helical content, concomitant with increased surface hydrophobicity; further, the apparent midpoint of temperature denaturation ($T_m$) drops considerably ($\Delta T_m = -24$ °C) [33,168], implying that EF-SAM oligomerization is intimately linked with the stability of the domain. It is, however, challenging to obtain high resolution structural detail of the $Ca^{2+}$-depleted dimer/oligomeric apo-state of EF-SAM due to sample heterogeneity, size and conformational exchange of the protein. NMR spectra of $Ca^{2+}$-free EF-SAM show limited number of peaks and narrow dispersion in the $^{1}H-^{15}N$ heteronuclear single quantum coherence (HSQC) [33,168,179], suggesting that the dimer/oligomer state is likely dynamic or in equilibrium with higher assembly states that would be invisible by NMR due to fast signal relaxation times. This spectrum is in stark contrast to the $Ca^{2+}$-loaded spectrum which shows well-dispersed peaks of homogeneous intensity, consistent with a well-folded monomeric structure. Interestingly, a recent biochemical study of $Ca^{2+}$-chelated EF-SAM demonstrated that an N-terminal helix-loop-helix (α6–α7) fragment resists proteolysis, suggesting that this region may be important in EF-SAM association [179].

Overall, the $Ca^{2+}$ sensing domain of STIMs have evolved whilst retaining the classical target recognition attribute found in many CaM superfamily members, which is characterized by a stably folded 'open' EF-hand architecture that exposes hydrophobic residues in the presence of $Ca^{2+}$ for interactions with hydrophobic residues of target proteins. In the absence of $Ca^{2+}$ ion, the STIM $Ca^{2+}$-sensing domain becomes destabilized and the resulting increased intrinsic disorder drives self-association in SOCE activation. Thus, whereas most CaM superfamily members undergo an 'open-to-closed' EF-hand response to the depletion of $Ca^{2+}$ which ultimately occludes target binding interfaces, STIMs have evolved an 'open/ordered-to-disordered' response to $Ca^{2+}$ depletion which results in homotypic interactions. Intrinsic protein disorder plays an important role in myriad cell signalling processes (*e.g.* Refs. [181–185]); STIMs use the EF-hand machinery to turn the disorder ON and OFF, which in turn acts as the ON/OFF activation switch for SOCE.

## 9. STIM1 cytoplasmic activation process

The act of EF-SAM luminal domain association triggers complex and dynamic structural changes in the cytoplasmic domains of STIM1, which culminates in the oligomerization, translocation to ER-PM junctions, binding to Orai1 subunits and gating of the channels [167,170,171,186–188]. First, the Lys-rich region is released as the CC1–CC2–CC3 domains undergo a conformational extension [189,190]. The Lys-rich region is involved in the

targeting of STIM1 molecules to ER-PM junctions through binding to negatively charged PM phosphoinositides [191–193]. However, in a separate mechanism of translocation, the CC2–CC3 domains, which constitute the minimal STIM machinery required to activate SOCE, interact with Orai1 N- and C-termini in the coupling and gating of the CRAC channel pore [170,171]. The mechanism of interaction between the Orai1 C-termini and the CC2 domain of STIM1 has been recently elucidated, revealing that the antiparallel orientation of the human Orai1 C-termini exhibited in the hexameric *Drosophila melanogaster* crystal structure [194] is remarkably analogous to the orientation after binding to the STIM-Orai association pocket (SOAP) formed exclusively by an antiparallel, intermolecular homotypic STIM1 CC2:CC2′ association [195]. The precise mechanism by which Orai1 N-termini interact with the CC2–CC3 region awaits further high resolution structural data. Note that intermolecular homotypic CC1–CC1′ interactions [196] as well as CC2–CC2′ interactions [197] have also been elucidated at high-resolution, and different relative conformations of CC1 and CC2 have been shown in NMR and crystal data [195]. These differences reinforce the notion of a dynamic coiled-coil switching mechanism of STIM1 activation and the marked intramolecular FRET, STIM localization and STIM mobility changes observed in the quiescent and active states [169,186–190,198,199].

## 10. STIM2 EF-SAM structure and function

Vertebrates express two human STIM homologues, STIM1 and STIM2. Although the activation mechanisms of STIM1 and STIM2 are likely similar considering the overall sequence conservation within the vital domains involved in $Ca^{2+}$ sensing (*i.e.* luminal EF-SAM) and activation (*i.e.* cytoplasmic CC1–CC2–CC3) of Orai (Fig. 4A), differences in the $Ca^{2+}$ sensitivity exist which tailor these molecules to specific physiological roles. For example, STIM2 becomes activated in response to smaller changes in ER $Ca^{2+}$ levels compared to STIM1, thus making it better suited to a role in the maintenance of basal $Ca^{2+}$ levels compared to STIM1 [166]. In contrast, STIM1 requires larger ER $Ca^{2+}$ store depletion to become activated compared to STIM2 [166,173]. These sensitivity differences are partially attributable to a lower $Ca^{2+}$ affinity of STIM2 compared to STIM1 [168,172,173]; however, high resolution structural data on STIM2 EF-SAM and biophysical characterizations have revealed additional factors involved in the homologue-specific roles in $Ca^{2+}$ signalling [173].

The high resolution structure of STIM2 EF-SAM revealed an overall secondary structure analogous to STIM1 EF-SAM, made up of 10 α-helices and 2 short β-strands (Fig. 6A). In 3D space, these components create a cEF (α1–β1–α2) and a ncEF (α3–β2–α4); further, a short linker helix (α5) connects the 5-helix SAM domain

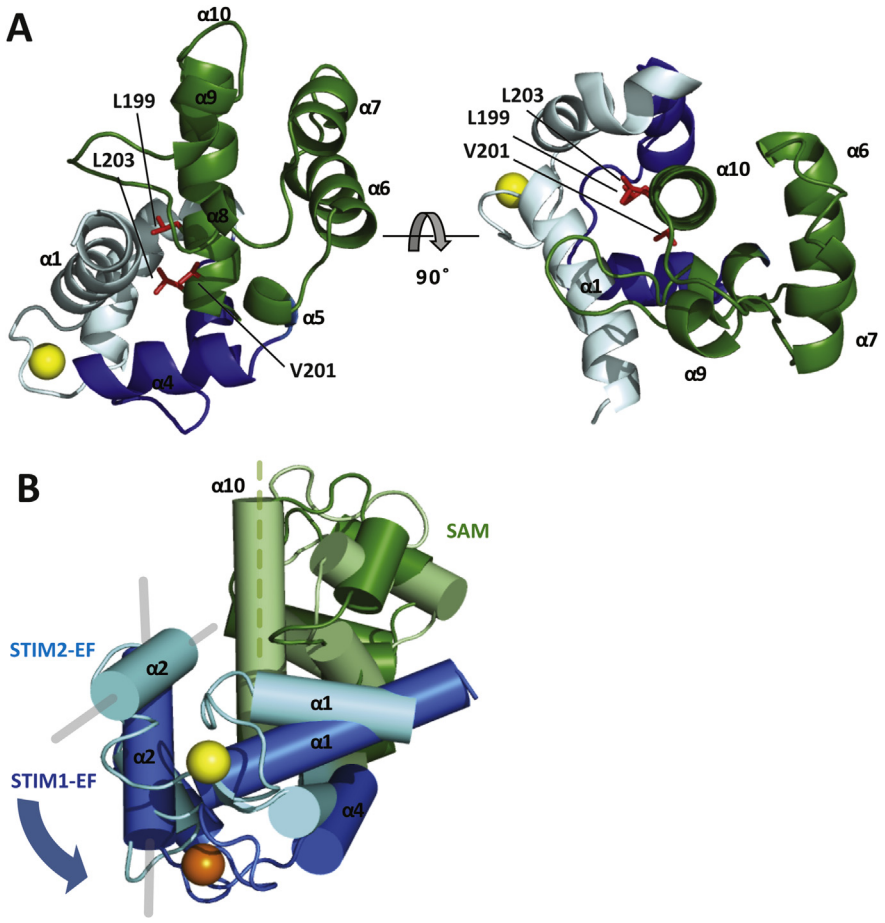


**Fig. 6.** STIM2 EF-SAM structural comparison with STIM1. (A) Solution structure of the STIM2 EF-SAM domain. The canonical EF-hand (cEF), non-canonical EF-hand (ncEF) and SAM domain are coloured light cyan, dark blue and dark green, respectively. The C-terminal anchor residues of the STIM2 SAM domain are shown as red sticks. The $Ca^{2+}$ ion is shown as a yellow sphere. The images were rendered in PyMOL using 2L5Y.pdb. (B) Backbone structural alignment of the STIM1 and STIM2 EF-SAM domains. The α10 helix of the STIM1 and STIM2 SAM domains are superimposed and the relative orientations of the STIM1 (light cyan) and STIM2 (dark blue) EF-hand domain are shown. The $Ca^{2+}$ ion coordinated by STIM1 (yellow) and STIM2 (orange) are shown as spheres. The images were rendered in PyMOL using 2K60.pdb and 2L5Y.pdb.

bundle (α6–α10) to the EF-hand pair (Fig. 6A). The EF-hand loops (β1 and β2) are stabilized through backbone H-bonding [*i.e.* Ile119 C(O):Ile 87 N(H)]; further, the SAM domain is anchored to a hydrophobic cleft formed by the EF-hand domain through α10 terminal hydrophobic residues, as also shown in the STIM1 EF-SAM structure (Fig. 5A) [33,173]. Despite the global similarities between the STIM1 and STIM2 EF-SAM structures, there are several unique features which contribute to the differences in $Ca^{2+}$ sensitivity (Fig. 6B). First, the EF-hand cleft of the STIM2 EF-SAM domain has more extensive hydrophobicity due to the inclusion of Lys103 and Trp128 within the pocket, whereas STIM1 excludes the homologous residues (*i.e.* His99 and Trp124). Second, the STIM2 SAM domain is further rotated away from the cEF compared to the SAM domain in STIM1. Third, oppositely charged Asp200 and Lys108 are in proximity and interact with each other in the STIM2 EF-SAM structure. Finally, the SAM domain of STIM2 has a more hydrophobic core compared to STIM1 due to the presence of Ile180 which is not conserved in STIM1 (*i.e.* Gly176 in STIM1); moreover, a rearrangement of the STIM2 SAM domain side chains to accommodate Ile180 results in the inclusion of Phe158 and Lys193 compared to Phe154 and Lys189, which are not included in the STIM1 SAM domain [173,200].

To assess the impact of the aforementioned EF-SAM structural distinctions on the $Ca^{2+}$ sensing function of the luminal domains, a series of STIM1/STIM2 EF-SAM chimeras were engineered and characterized *in vitro* and in live cells after incorporation in the full-length STIM1 context. Compared to STIM1, wild-type STIM2 EF-SAM shows a decreased tendency to dimerize and oligomerize, consistent with an increased overall stability in both the $Ca^{2+}$-loaded and −depleted states [173,201]. Remarkably, both 'superstable' and 'superunstable' STIM1/STIM2 EF-SAM chimeras were created; moreover, a fusion consisting of the STIM2 cEF, the STIM1 ncEF and the STIM1 SAM domain (*i.e.* ES211) showed markedly decreased stability in the respective $Ca^{2+}$-loaded and -depleted states compared with wild-type STIM1 or STIM2 EF-SAM. On the other hand, a fusion comprised of the STIM1 cEF, STIM2 ncEF and STIM2 SAM domain (*i.e.* ES122) was more stable than wild-type STIM1 or STIM2 EF-SAM in the respective $Ca^{2+}$-loaded and −depleted states [173]. The replacement of EF-SAM with ES211 (*i.e.* superunstable) in full-length STIM1 resulted in constitutive puncta (*i.e.* oligomerized STIM1 at ER-PM junctions) and open CRAC channels; moreover, incorporating ES122 (*i.e.* superstable) in the place of wild-type EF-SAM resulted in a STIM1 molecule with a significantly delayed time to maximal activation and highly suppressed maximal CRAC activity [173]. These data were instrumental in unequivocally linking the stability of the EF-SAM region to the activation of the full-length molecule.

## 11. Disease-associated STIM1 mutations

The PM protein subunit Orai1 that makes up the CRAC channel was identified through a gene linkage analysis of a family carrying a heritable form of severe combined immunodeficiency disease (SCID) characterized by a lack of SOCE; moreover, the analysis identified Orai1 as a major protein component of SOCE machinery and the R91W as the mutation within Orai1 responsible for the SCID phenotype [202]. There is no alteration in the expression levels of Orai1 R91W in immune cells from human patients, but these cells show no detectable SOCE, a phenotype which can only be rescued by overexpression of wild-type Orai1 [202]. Since the identification of Orai1 R91W, several other germline mutations in both Orai1 and STIM1 have been found associated with immunodeficiency diseases. The deficiency occurs in both the innate and adaptive immune systems and patients exhibit a high susceptibility to bacterial, viral and fungal pathogens [203,204]. Within Orai1, a frameshift mutation (A88SfsX25) as well as the missense A103E and L194P have been shown to abolish protein levels and CRAC activity [205–207] in families exhibiting immunodeficiency disease [203]. Two classes of heritable mutations in STIM1 have also been found in human immunodeficient patients. In the first class, STIM1 protein expression is abrogated due to frameshift (E128RfsX9) or splice site (1538−1 G to A) mutations, resulting in a loss of SOCE [208,209]. In the second class, missense mutations do not alter STIM1 protein levels compared to normal individuals, but STIM1 function is lost nonetheless as cells from patients with these mutations also show no SOCE and develop immunodeficiency-like disease (*i.e.* R429C) [210,211].

Remarkably, whereas the above described mutations result in a loss of SOCE and immunodeficiency, recently two independent groups identified an autosomal dominantly inherited STIM1 mutation (R304W) which causes Stormorken syndrome, a condition characterized by bleeding dysfunction, tubular aggregates, intellectual disability and skin abnormalities; however, SOCE is constitutively active in cells expressing STIM1 R304W [212,213]. Thus, both loss- and gain-of-function mutations in STIM1 can lead to diseases acquired through a Mendelian-inheritance pattern which causing a range of abnormal phenotypes. Note that somatic STIM1 coding point mutations (*i.e.* currently 80 listed in the COSMIC database [214]) have also been identified associated with various cancers, although the functional consequences of these mutants are not well understood.

## 12. Concluding remarks

The structural versatility of CaM involves the presence of a flexible linker between the N- and C-terminal EF-hand domains permitting CaM to change its global shape and adapt to the binding sites of different target proteins; further, the hydrophobic cleft of each EF-hand domain is highly enriched with methionine which has electrostatically semi-polar and structurally flexible properties. Thus, not only does the dynamic linker facilitate a global conformational adaption, but the individual side chains making up the cleft are capable of local adjustments to the precise positions and properties of target anchor residues. Taken together with a $Ca^{2+}$ binding affinity which is specifically tuned to the range of $Ca^{2+}$ levels experienced by the cytoplasm (*i.e.* 0.1–1 μM), CaM can regulate diverse, spatio-temporally distinct signalling processes in response to global and local changes in cytoplasmic $Ca^{2+}$ levels. In the ER, another class of $Ca^{2+}$ sensors has been identified in the STIMs, which have adapted to the much higher $Ca^{2+}$ level of the ER lumen (*i.e.* 0.1–1 mM). The balance between $Ca^{2+}$ affinity and SAM stability make STIM1 well suited to SOCE regulation and STIM2 to basal $Ca^{2+}$ homeostatis.

Although the general EF-hand cleft:hydrophobic anchor mechanism of target recognition is conserved between STIM1, STIM2 and CaM, STIMs and CaM exhibit several intriguing variations in mechanisms of action (see Table 1 in Ref. [215]). STIMs possess 1 canonical $Ca^{2+}$ binding EF-hand paired with 1 non-canonical EF-hand, while CaM has evolved 4 canonical EF-hands, each of which are capable of binding $Ca^{2+}$ with differing levels of affinity (*i.e.* weak affinity STIMs versus high affinity CaM). In the $Ca^{2+}$-loaded state, STIMs and CaM maintain open EF-hand conformations. Remarkably, however, open EF-hands maintain STIM in a monomeric state, while CaM with open EF-hands habitually binds to targets, thereby forming heteromeric complexes. In the $Ca^{2+}$-depleted state, STIMs show increased hydrophobicity associated with oligomerization, while the closed EF-hand motifs of CaM exhibit decreased hydrophobicity. Most fascinatingly, the origin of regulatory diversity for STIMs occurs through genetic polymorphism, while CaM employs a conformational plasticity.

Despite the intriguing variations, the function of STIMs and CaM are not totally mutually exclusive. CaM can bind to the cytosolic domains of both STIM1 and STIM2 and may play a role in targeting of STIMs to ER-PM junctions or in disassembling STIMs from Orai proteins during inactivation [216]. The binding sites on STIM1 and STIM2 are located at the far C-terminus of the molecules (*i.e.* residues 667–685 and residues 730–746, respectively) [216] and each contain potential hydrophobic anchor residues. Additionally, CaM has been shown to bind to the N-terminal gating helix of Orai1 and is associated with $Ca^{2+}$-dependent inactivation of SOCE [217]. A crystal structure of $Ca^{2+}$–CaM shows the Orai1 N-terminal domain peptide localized in the CaM C-terminal domain hydrophobic cleft, and additional solution studies reveal that the CaM N-terminal domain is also capable of separately binding the Orai1 N-terminal domain peptide with lower affinity; hence, CaM binds to Orai1 in 1:2 stoichiometry, respectively, which has implications for controlling the functional oligomerization state of Orai1 [218].

Additionally, a cooperative role between STIM1 and STIM2 in transducing ER $Ca^{2+}$ signals cannot be discounted and is likely considering the co-localization within various cell types. However, precisely how STIM1 and STIM2 may cooperate as ER $Ca^{2+}$ sensors in luminal-dependent signalling processes requires further studies on the ability of these proteins to interact, the physicochemical basis for the interactions and the influence of the communication on the function of each respective protein.

A decade ago CaM mutations associated with human disease were believed to be unlikely as this regulator was considered to be too essential to be functionally altered in the cell. Remarkably, recent DNA sequencing efforts have uncovered a number of mutations in CaM which result in dangerous cardiac arrhythmias. Cancer sequencing projects have also revealed numerous missense mutations in CaM that occur at the somatic level. Similarly, STIM1 has been shown to be mutated in familial immunodeficiency-associated diseases and Stormorken syndromes and somatically in cancers. Clinical studies which identify disease-related mutations are invaluable to understanding the structure-function relationships of these $Ca^{2+}$ sensor proteins, and as further mutational data are collected from patients and this genomic information is linked to cellular, molecular and structural biological data, a better understanding of the mechanisms of $Ca^{2+}$-signalling malignancies will come to light and lead to important new therapeutic strategies for treatments.

## Conflict of interest

The authors declare no conflict of interest.

## Acknowledgments

This work was supported by the Canadian Institutes of Health Research (Grant #MOP 13552 to MI), the Heart and Stroke Foundation of Canada (Grant #'s G130001814 and T7181 to MI) and the Natural Sciences and Engineering Research Council of Canada (Grant #UT493093 to MI and #201405239 to PBS). MI holds the Canada Research Chair in Cancer Structural Biology.

## Transparency document

Transparency document related to this article can be found online at http://dx.doi.org/10.1016/j.bbrc.2015.01.106.

## References

[1] W.Y. Cheung, Cyclic 3′,5′-nucleotide phosphodiesterase. Demonstration of an activator, Biochem. Biophys. Res. Commun. 38 (1970) 533–538.
[2] S. Kakiuchi, R. Yamazaki, Calcium dependent phosphodiesterase activity and its activating factor (PAF) from brain studies on cyclic 3′,5′-nucleotide phosphodiesterase (3), Biochem. Biophys. Res. Commun. 41 (1970) 1104–1110.
[3] C.O. Brostrom, Y.C. Huang, B.M. Breckenridge, D.J. Wolff, Identification of a calcium-binding protein as a calcium-dependent regulator of brain adenylate cyclase, Proc. Natl. Acad. Sci. U. S. A. 72 (1975) 64–68.
[4] R.M. Gopinath, F.F. Vincenzi, Phosphodiesterase protein activator mimics red blood cell cytoplasmic activator of (Ca2+–Mg2+)ATPase, Biochem. Biophys. Res. Commun. 77 (1977) 1203–1209.
[5] H.W. Jarrett, J.T. Penniston, Partial purification of the Ca2+–Mg2+ ATPase activator from human erythrocytes: its similarity to the activator of 3′:5′ – cyclic nucleotide phosphodiesterase, Biochem. Biophys. Res. Commun. 77 (1977) 1210–1216.
[6] M. Yazawa, K. Yagi, Calcium-binding subunit of myosin light chain kinase, J. Biochem. 82 (1977) 287–289.
[7] E. Carafoli, C.B. Klee, Calcium as a Cellular Regulator, Oxford University Press, New York, 1999.
[8] H. Hidaka, D.J. Hartshorne, Calmodulin Antagonists and Cellular Physiology, Academic Press, Orlando, 1985.
[9] H. Tidow, P. Nissen, Structural diversity of calmodulin binding to its target sites, FEBS J. 280 (2013) 5551–5565.
[10] K.P. Hoeflich, M. Ikura, Calmodulin in action: diversity in target recognition and activation mechanisms, Cell 108 (2002) 739–742.
[11] R.R. Copley, J. Schultz, C.P. Ponting, P. Bork, Protein families in multicellular organisms, Curr. Opin. Struct. Biol. 9 (1999) 408–415.
[12] M. Ikura, J.B. Ames, Genetic polymorphism and protein conformational plasticity in the calmodulin superfamily: two ways to promote multifunctionality, Proc. Natl. Acad. Sci. U. S. A. 103 (2006) 1159–1164.
[13] R.H. Kretsinger, V.N. Uversky, E.A. Permyakov, Encyclopedia of Metalloproteins, Springer, New York, 2013.
[14] L.J. Van Eldik, D.M. Watterson, Calmodulin and Signal Transduction, Academic Press, San Diego, 1998.
[15] K.L. Yap, J. Kim, K. Truong, M. Sherman, T. Yuan, M. Ikura, Calmodulin target database, J. Struct. Funct. Genomics 1 (2000) 8–14.
[16] J.B. Ames, S. Lim, Molecular structure and target recognition of neuronal calcium sensor proteins, Biochim. Biophys. Acta 1820 (2012) 1205–1213.
[17] S. Bhattacharya, C.G. Bunick, W.J. Chazin, Target selectivity in EF-hand calcium binding proteins, Biochim. Biophys. Acta 1742 (2004) 69–79.
[18] J.L. Gifford, M.P. Walsh, H.J. Vogel, Structures and metal-ion-binding properties of the Ca2+-binding helix-loop-helix EF-hand motifs, Biochem. J. 405 (2007) 199–221.
[19] Z. Grabarek, Insights into modulation of calcium signaling by magnesium in calmodulin, troponin C and related EF-hand proteins, Biochim. Biophys. Acta 1813 (2011) 913–921.
[20] A. Hermann, R. Donato, T.M. Weiger, W.J. Chazin, S100 calcium binding proteins and ion channels, Front. Pharmacol. 3 (2012) 67.
[21] B. Schwaller, Cytosolic Ca2+ buffers, Cold Spring Harb. Perspect. Biol. 2 (2010) a004051.
[22] J.W. Putney Jr., A model for receptor-regulated calcium entry, Cell Calcium 7 (1986) 1–12.
[23] H.E. Collins, X. Zhu-Mauldin, R.B. Marchase, J.C. Chatham, STIM1/Orai1-mediated SOCE: current perspectives and potential roles in cardiac function and pathology, Am. J. Physiol. Heart Circ. Physiol. 305 (2013) H446–H458.
[24] S. Feske, E.Y. Skolnik, M. Prakriya, Ion channels and transporters in lymphocyte function and immunity, Nat. Rev. Immunol. 12 (2012) 532–547.
[25] J. Gruszczynska-Biegala, J. Kuznicki, Native STIM2 and ORAI1 proteins form a calcium-sensitive and thapsigargin-insensitive complex in cortical neurons, J. Neurochem. 126 (2013) 727–738.
[26] R. Hooper, B.S. Rothberg, J. Soboloff, Neuronal STIMulation at rest, Sci. Signal. 7 (2014) pe18.
[27] P.J. Shaw, S. Feske, Physiological and pathophysiological functions of SOCE in the immune system, Front. Biosci. (Elite Ed) 4 (2012) 2253–2268.
[28] J. Liou, M.L. Kim, W.D. Heo, J.T. Jones, J.W. Myers, J.E. Ferrell Jr., T. Meyer, STIM is a Ca2+ sensor essential for Ca2+-store-depletion-triggered Ca2+ influx, Curr. Biol. 15 (2005) 1235–1241.
[29] J. Roos, P.J. DiGregorio, A.V. Yeromin, K. Ohlsen, M. Lioudyno, S. Zhang, O. Safrina, J.A. Kozak, S.L. Wagner, M.D. Cahalan, G. Velicelebi, K.A. Stauderman, STIM1, an essential and conserved component of store-operated Ca2+ channel function, J. Cell Biol. 169 (2005) 435–445. Epub 2005 May 2002.
[30] Y.S. Babu, C.E. Bugg, W.J. Cook, Structure of calmodulin refined at 2.2 A resolution, J. Mol. Biol. 204 (1988) 191–204.
[31] O. Herzberg, M.N. James, Structure of the calcium regulatory muscle protein troponin-C at 2.8 A resolution, Nature 313 (1985) 653–659.
[32] R.H. Kretsinger, C.E. Nockolds, Carp muscle calcium-binding protein. II. Structure determination and general description, J. Biol. Chem. 248 (1973) 3313–3326.
[33] P.B. Stathopulos, L. Zheng, G.Y. Li, M.J. Plevin, M. Ikura, Structural and mechanistic insights into STIM1-mediated initiation of store-operated calcium entry, Cell 135 (2008) 110–122.
[34] Y.S. Babu, J.S. Sack, T.J. Greenhough, C.E. Bugg, A.R. Means, W.J. Cook, Three-dimensional structure of calmodulin, Nature 315 (1985) 37–40.
[35] M.J. Berridge, P. Lipp, M.D. Bootman, The versatility and universality of calcium signalling, Nat. Rev. Mol. Cell Biol. 1 (2000) 11–21.

[36] M.D. Bootman, O.H. Petersen, A. Verkhratsky, The endoplasmic reticulum is a focal point for co-ordination of cellular activity, Cell Calcium 32 (2002) 231–234.
[37] S. Linse, A. Helmersson, S. Forsen, Calcium binding to calmodulin and its globular domains, J. Biol. Chem. 266 (1991) 8050–8054.
[38] P.M. Bayley, W.A. Findlay, S.R. Martin, Target recognition by calmodulin: dissecting the kinetics and affinity of interaction using short peptide sequences, Protein Sci. 5 (1996) 1215–1228.
[39] G. Barbato, M. Ikura, L.E. Kay, R.W. Pastor, A. Bax, Backbone dynamics of calmodulin studied by 15N relaxation using inverse detected two-dimensional NMR spectroscopy: the central helix is flexible, Biochemistry 31 (1992) 5269–5278.
[40] M. Ikura, L.E. Kay, A. Bax, A novel approach for sequential assignment of 1H, 13C, and 15N spectra of proteins: heteronuclear triple-resonance three-dimensional NMR spectroscopy. Application to calmodulin, Biochemistry 29 (1990) 4659–4667.
[41] M. Ikura, L.E. Kay, M. Krinks, A. Bax, Triple-resonance multidimensional NMR study of calmodulin complexed with the binding domain of skeletal muscle myosin light-chain kinase: indication of a conformational change in the central helix, Biochemistry 30 (1991) 5498–5504.
[42] B.E. Finn, J. Evenas, T. Drakenberg, J.P. Waltho, E. Thulin, S. Forsen, Calcium-induced structural changes and domain autonomy in calmodulin, Nat. Struct. Biol. 2 (1995) 777–783.
[43] H. Kuboniwa, N. Tjandra, S. Grzesiek, H. Ren, C.B. Klee, A. Bax, Solution structure of calcium-free calmodulin, Nat. Struct. Biol. 2 (1995) 768–776.
[44] M. Zhang, T. Tanaka, M. Ikura, Calcium-induced conformational transition revealed by the solution structure of apo calmodulin, Nat. Struct. Biol. 2 (1995) 758–767.
[45] H.J. Vogel, M. Zhang, Protein engineering and NMR studies of calmodulin, Mol. Cell. Biochem. 149–150 (1995) 3–15.
[46] A. Villarroel, M. Taglialatela, G. Bernardo-Seisdedos, A. Alaimo, J. Agirre, A. Alberdi, C. Gomis-Perez, M.V. Soldovieri, P. Ambrosino, C. Malo, P. Areso, The ever changing moods of calmodulin: how structural plasticity entails transductional adaptability, J. Mol. Biol. 426 (2014) 2717–2735.
[47] R. Buratti, G. Prestipino, P. Menegazzi, S. Treves, F. Zorzato, Calcium dependent activation of skeletal muscle Ca2+ release channel (ryanodine receptor) by calmodulin, Biochem. Biophys. Res. Commun. 213 (1995) 1082–1090.
[48] O. Fuentes, C. Valdivia, D. Vaughan, R. Coronado, H.H. Valdivia, Calcium-dependent block of ryanodine receptor channel of swine skeletal muscle by direct binding of calmodulin, Cell Calcium 15 (1994) 305–316.
[49] T. Ikemoto, M. Iino, M. Endo, Enhancing effect of calmodulin on Ca(2+)-induced Ca2+ release in the sarcoplasmic reticulum of rabbit skeletal muscle fibres, J. Physiol. 487 (Pt. 3) (1995) 573–582.
[50] A. Tripathy, L. Xu, G. Mann, G. Meissner, Calmodulin activation and inhibition of skeletal muscle Ca2+ release channel (ryanodine receptor), Biophys. J. 69 (1995) 106–119.
[51] K. Lau, M.M. Chan, F. Van Petegem, Lobe-specific calmodulin binding to different ryanodine receptor isoforms, Biochemistry 53 (2014) 932–946.
[52] C.E. Adkins, S.A. Morris, H. De Smedt, I. Sienaert, K. Torok, C.W. Taylor, Ca2+-calmodulin inhibits Ca2+ release mediated by type-1, -2 and -3 inositol trisphosphate receptors, Biochem. J. 345 (Pt. 2) (2000) 357–363.
[53] T. Michikawa, J. Hirota, S. Kawano, M. Hiraoka, M. Yamada, T. Furuichi, K. Mikoshiba, Calmodulin mediates calcium-dependent inactivation of the cerebellar type 1 inositol 1,4,5-trisphosphate receptor, Neuron 23 (1999) 799–808.
[54] L. Missiaen, H. DeSmedt, G. Bultynck, S. Vanlingen, P. Desmet, G. Callewaert, J.B. Parys, Calmodulin increases the sensitivity of type 3 inositol-1,4, 5-trisphosphate receptors to Ca(2+) inhibition in human bronchial mucosal cells, Mol. Pharmacol. 57 (2000) 564–567.
[55] T.J. Cardy, C.W. Taylor, A novel role for calmodulin: Ca2+-independent inhibition of type-1 inositol trisphosphate receptors, Biochem. J. 334 (Pt. 2) (1998) 447–455.
[56] S. Patel, S.A. Morris, C.E. Adkins, G. O'Beirne, C.W. Taylor, Ca2+-independent inhibition of inositol trisphosphate receptors by calmodulin: redistribution of calmodulin as a possible means of regulating Ca2+ mobilization, Proc. Natl. Acad. Sci. U. S. A. 94 (1997) 11627–11632.
[57] S. Kang, H. Kwon, H. Wen, Y. Song, D. Frueh, H.C. Ahn, S.H. Yoo, G. Wagner, S. Park, Global dynamic conformational changes in the suppressor domain of IP3 receptor by stepwise binding of the two lobes of calmodulin, FASEB J. 25 (2011) 840–850.
[58] B. Elshorst, M. Hennig, H. Forsterling, A. Diener, M. Maurer, P. Schulte, H. Schwalbe, C. Griesinger, J. Krebs, H. Schmid, T. Vorherr, E. Carafoli, NMR solution structure of a complex of calmodulin with a binding peptide of the Ca2+ pump, Biochemistry 38 (1999) 12320–12332.
[59] D. Guerini, J. Krebs, E. Carafoli, Stimulation of the purified erythrocyte Ca2+-ATPase by tryptic fragments of calmodulin, J. Biol. Chem. 259 (1984) 15172–15177.
[60] M. Kataoka, J.F. Head, T. Vorherr, J. Krebs, E. Carafoli, Small-angle X-ray scattering study of calmodulin bound to two peptides corresponding to parts of the calmodulin-binding domain of the plasma membrane Ca2+ pump, Biochemistry 30 (1991) 6247–6251.
[61] A.R. Penheiter, A.G. Filoteo, J.T. Penniston, A.J. Caride, Kinetic analysis of the calmodulin-binding region of the plasma membrane calcium pump isoform 4b, Biochemistry 44 (2005) 2009–2020.
[62] A.K. Verma, A.G. Filoteo, D.R. Stanford, E.D. Wieben, J.T. Penniston, E.E. Strehler, R. Fischer, R. Heim, G. Vogel, S. Mathews, et al., Complete primary structure of a human plasma membrane Ca2+ pump, J. Biol. Chem. 263 (1988) 14152–14159.
[63] N. Juranic, E. Atanasova, A.G. Filoteo, S. Macura, F.G. Prendergast, J.T. Penniston, E.E. Strehler, Calmodulin wraps around its binding domain in the plasma membrane Ca2+ pump anchored by a novel 18-1 motif, J. Biol. Chem. 285 (2010) 4015–4024.
[64] M.G. Erickson, H. Liang, M.X. Mori, D.T. Yue, FRET two-hybrid mapping reveals function and location of L-type Ca2+ channel CaM preassociation, Neuron 39 (2003) 97–107.
[65] A.P. Yamniuk, H.J. Vogel, Calmodulin's flexibility allows for promiscuity in its interactions with target proteins and peptides, Mol. Biotechnol. 27 (2004) 33–57.
[66] M. Ikura, G.M. Clore, A.M. Gronenborn, G. Zhu, C.B. Klee, A. Bax, Solution structure of a calmodulin-target peptide complex by multidimensional NMR, Science 256 (1992) 632–638.
[67] W.E. Meador, A.R. Means, F.A. Quiocho, Target enzyme recognition by calmodulin: 2.4 A structure of a calmodulin-peptide complex, Science 257 (1992) 1251–1255.
[68] A.R. Rhoads, F. Friedberg, Sequence motifs for calmodulin recognition, FASEB J. 11 (1997) 331–340.
[69] W.E. Meador, A.R. Means, F.A. Quiocho, Modulation of calmodulin plasticity in molecular recognition on the basis of x-ray structures, Science 262 (1993) 1718–1721.
[70] M. Osawa, H. Tokumitsu, M.B. Swindells, H. Kurihara, M. Orita, T. Shibanuma, T. Furuya, M. Ikura, A novel target recognition revealed by calmodulin in complex with Ca2+-calmodulin-dependent kinase kinase, Nat. Struct. Biol. 6 (1999) 819–824.
[71] E. Franco-Echevarria, J.I. Banos-Sanz, B. Monterroso, A. Round, J. Sanz-Aparicio, B. Gonzalez, A new calmodulin-binding motif for inositol 1,4,5-trisphosphate 3-kinase regulation, Biochem. J. 463 (2014) 319–328.
[72] A.A. Maximciuc, J.A. Putkey, Y. Shamoo, K.R. Mackenzie, Complex of calmodulin with a ryanodine receptor target reveals a novel, flexible binding mode, Structure 14 (2006) 1547–1556.
[73] H. Ishida, H.J. Vogel, The solution structure of a plant calmodulin and the CaM-binding domain of the vacuolar calcium-ATPase BCA1 reveals a new binding and activation mechanism, J. Biol. Chem. 285 (2010) 38502–38510.
[74] H. Tidow, L.R. Poulsen, A. Andreeva, M. Knudsen, K.L. Hein, C. Wiuf, M.G. Palmgren, P. Nissen, A bimodular mechanism of calcium control in eukaryotes, Nature 491 (2012) 468–472.
[75] E. Yamauchi, T. Nakatsu, M. Matsubara, H. Kato, H. Taniguchi, Crystal structure of a MARCKS peptide containing the calmodulin-binding domain in complex with Ca2+-calmodulin, Nat. Struct. Biol. 10 (2003) 226–231.
[76] K.L. Yap, T. Yuan, T.K. Mal, H.J. Vogel, M. Ikura, Structural basis for simultaneous binding of two carboxy-terminal peptides of plant glutamate decarboxylase to calmodulin, J. Mol. Biol. 328 (2003) 193–204.
[77] Q. Ye, X. Li, A. Wong, Q. Wei, Z. Jia, Structure of calmodulin bound to a calcineurin peptide: a new way of making an old binding mode, Biochemistry 45 (2006) 738–745.
[78] V. Majava, P. Kursula, Domain swapping and different oligomeric states for the complex between calmodulin and the calmodulin-binding domain of calcineurin a, PLoS One 4 (2009) e5402.
[79] T.B. Dunlap, H.F. Guo, E.C. Cook, E. Holbrook, J. Rumi-Masante, T.E. Lester, C.L. Colbert, C.W. Vander Kooi, T.P. Creamer, Stoichiometry of the calcineurin regulatory domain-calmodulin complex, Biochemistry 53 (2014) 5779–5790.
[80] E.M. Espreafico, R.E. Cheney, M. Matteoli, A.A. Nascimento, P.V. De Camilli, R.E. Larson, M.S. Mooseker, Primary structure and cellular localization of chicken brain myosin-V (p190), an unconventional myosin with calmodulin light chains, J. Cell Biol. 119 (1992) 1541–1557.
[81] J. Ruan, Q. Xie, N. Hutchinson, H. Cho, G.C. Wolfe, C. Nathan, Inducible nitric oxide synthase requires both the canonical calmodulin-binding domain and additional sequences in order to bind calmodulin and produce nitric oxide in the absence of free Ca2+, J. Biol. Chem. 271 (1996) 22679–22686.
[82] T. Yuan, M.P. Walsh, C. Sutherland, H. Fabian, H.J. Vogel, Calcium-dependent and -independent interactions of the calmodulin-binding domain of cyclic nucleotide phosphodiesterase with calmodulin, Biochemistry 38 (1999) 1446–1455.
[83] M. Dasgupta, T. Honeycutt, D.K. Blumenthal, The gamma-subunit of skeletal muscle phosphorylase kinase contains two noncontiguous domains that act in concert to bind calmodulin, J. Biol. Chem. 264 (1989) 17156–17163.
[84] J. Baudier, J.C. Deloulme, A. Van Dorsselaer, D. Black, H.W. Matthes, Purification and characterization of a brain-specific protein kinase C substrate, neurogranin (p17). Identification of a consensus amino acid sequence between neurogranin and neuromodulin (GAP43) that corresponds to the protein kinase C phosphorylation site and the calmodulin-binding domain, J. Biol. Chem. 266 (1991) 229–237.
[85] S. Pathmanathan, E. Hamilton, E. Atcheson, D.J. Timson, The interaction of IQGAPs with calmodulin-like proteins, Biochem. Soc. Trans. 39 (2011) 694–699.
[86] A. Houdusse, J.F. Gaucher, E. Krementsova, S. Mui, K.M. Trybus, C. Cohen, Crystal structure of apo-calmodulin bound to the first two IQ motifs of myosin V reveals essential recognition features, Proc. Natl. Acad. Sci. U. S. A. 103 (2006) 19326–19331.
[87] M.D. Feldkamp, L. Yu, M.A. Shea, Structural and energetic determinants of apo calmodulin binding to the IQ motif of the Na(V)1.2 voltage-dependent sodium channel, Structure 19 (2011) 733–747.

[88] B. Chagot, W.J. Chazin, Solution NMR structure of apo-calmodulin in complex with the IQ motif of human cardiac sodium channel NaV1.5, J. Mol. Biol. 406 (2011) 106–119.

[89] C. Wang, B.C. Chung, H. Yan, H.G. Wang, S.Y. Lee, G.S. Pitt, Structural analyses of Ca(2)(+)/CaM interaction with NaV channel C-termini reveal mechanisms of calcium-dependent regulation, Nat. Commun. 5 (2014) 4896.

[90] F. Van Petegem, F.C. Chatelain, D.L. Minor Jr., Insights into voltage-gated calcium channel regulation from the structure of the CaV1.2 IQ domain-Ca2+/calmodulin complex, Nat. Struct. Mol. Biol. 12 (2005) 1108–1115.

[91] J.L. Fallon, D.B. Halling, S.L. Hamilton, F.A. Quiocho, Structure of calmodulin bound to the hydrophobic IQ domain of the cardiac Ca(v)1.2 calcium channel, Structure 13 (2005) 1881–1886.

[92] E.Y. Kim, C.H. Rumpf, Y. Fujiwara, E.S. Cooley, F. Van Petegem, D.L. Minor Jr., Structures of CaV2 Ca2+/CaM-IQ domain complexes reveal binding modes that underlie calcium-dependent inactivation and facilitation, Structure 16 (2008) 1455–1467.

[93] V. Kumar, V.P. Chichili, L. Zhong, X. Tang, A. Velazquez-Campoy, F.S. Sheu, J. Seetharaman, N.Z. Gerges, J. Sivaraman, Structural basis for the interaction of unstructured neuron specific substrates neuromodulin and neurogranin with calmodulin, Sci. Rep. 3 (2013) 1392.

[94] D. Chin, A.R. Means, Calmodulin: a prototypical calcium sensor, Trends Cell Biol. 10 (2000) 322–328.

[95] G. Manning, D.B. Whyte, R. Martinez, T. Hunter, S. Sudarsanam, The protein kinase complement of the human genome, Science 298 (2002) 1912–1934.

[96] J. Aramburu, A. Rao, C.B. Klee, Calcineurin: from structure to function, Curr. Top. Cell. Regul. 36 (2000) 237–295.

[97] C.B. Klee, G.F. Draetta, M.J. Hubbard, Calcineurin, Adv. Enzymol. Relat. Areas Mol. Biol. 61 (1988) 149–200.

[98] F. Rusnak, P. Mertz, Calcineurin: form and function, Physiol. Rev. 80 (2000) 1483–1521.

[99] A. Crivici, M. Ikura, Molecular and structural basis of target recognition by calmodulin, Annu. Rev. Biophys. Biomol. Struct. 24 (1995) 85–116.

[100] I. de Diego, J. Kuper, N. Bakalova, P. Kursula, M. Wilmanns, Molecular basis of the death-associated protein kinase-calcium/calmodulin regulator complex, Sci. Signal. 3 (2010) ra6.

[101] Y. Lai, A.C. Nairn, P. Greengard, Autophosphorylation reversibly regulates the Ca2+/calmodulin-dependence of Ca2+/calmodulin-dependent protein kinase II, Proc. Natl. Acad. Sci. U. S. A. 83 (1986) 4253–4257.

[102] S.G. Miller, M.B. Kennedy, Regulation of brain type II Ca2+/calmodulin-dependent protein kinase by autophosphorylation: a Ca2+-triggered molecular switch, Cell 44 (1986) 861–870.

[103] K. Shen, T. Meyer, Dynamic control of CaMKII translocation and localization in hippocampal neurons by NMDA receptor stimulation, Science 284 (1999) 162–166.

[104] S.J. Coultrap, K. Barcomb, K.U. Bayer, A significant but rather mild contribution of T286 autophosphorylation to Ca2+/CaM-stimulated CaMKII activity, PLoS One 7 (2012) e37176.

[105] T. Meyer, P.I. Hanson, L. Stryer, H. Schulman, Calmodulin trapping by calcium-calmodulin dependent protein-kinase, Science 256 (1992) 1199–1202.

[106] S.I. Singla, A. Hudmon, J.M. Goldberg, J.L. Smith, H. Schulman, Molecular characterization of calmodulin trapping by calcium/calmodulin-dependent protein kinase II, J. Biol. Chem. 276 (2001) 29353–29360.

[107] M.M. Stratton, L.H. Chao, H. Schulman, J. Kuriyan, Structural studies on the regulation of Ca2+/calmodulin dependent protein kinase II, Curr. Opin. Struct. Biol. 23 (2013) 292–301.

[108] L.H. Chao, M.M. Stratton, I.H. Lee, O.S. Rosenberg, J. Levitz, D.J. Mandell, T. Kortemme, J.T. Groves, H. Schulman, J. Kuriyan, A mechanism for tunable autoinhibition in the structure of a human Ca2+/calmodulin- dependent kinase II holoenzyme, Cell 146 (2011) 732–745.

[109] O.S. Rosenberg, S. Deindl, R.J. Sung, A.C. Nairn, J. Kuriyan, Structure of the autoinhibited kinase domain of CaMKII and SAXS analysis of the holoenzyme, Cell 123 (2005) 849–860.

[110] P. Rellos, A.C. Pike, F.H. Niesen, E. Salah, W.H. Lee, F. von Delft, S. Knapp, Structure of the CaMKIIdelta/calmodulin complex reveals the molecular mechanism of CaMKII kinase activation, PLoS Biol. 8 (2010) e1000426.

[111] R.J. Colbran, T.R. Soderling, Calcium/calmodulin-independent autophosphorylation sites of calcium/calmodulin-dependent protein kinase II. Studies on the effect of phosphorylation of threonine 305/306 and serine 314 on calmodulin binding using synthetic peptides, J. Biol. Chem. 265 (1990) 11213–11219.

[112] Q. Huai, H.Y. Kim, Y.D. Liu, Y.D. Zhao, A. Mondragon, J.O. Liu, H.M. Ke, Crystal structure of calcineurin-cyclophilin-cyclosporin shows common but distinct recognition of immunophilin-drug complexes, Proc. Natl. Acad. Sci. U. S. A. 99 (2002) 12037–12042.

[113] L. Jin, S.C. Harrison, Crystal structure of human calcineurin complexed with cyclosporin A and human cyclophilin, Proc. Natl. Acad. Sci. U. S. A. 99 (2002) 13522–13526.

[114] P.M. Stemmer, C.B. Klee, Dual calcium-ion regulation of calcineurin by calmodulin and calcineurin-B, Biochemistry 33 (1994) 6859–6866.

[115] C. Xia, I. Misra, T. Iyanagi, J.J. Kim, Regulation of interdomain interactions by calmodulin in inducible nitric-oxide synthase, J. Biol. Chem. 284 (2009) 30708–30717.

[116] C.L. Drum, S.Z. Yan, J. Bard, Y.Q. Shen, D. Lu, S. Soelaiman, Z. Grabarek, A. Bohm, W.J. Tang, Structural basis for the activation of anthrax adenylyl cyclase exotoxin by calmodulin, Nature 415 (2002) 396–402.

[117] M.A. Schumacher, A.F. Rivard, H.P. Bachinger, J.P. Adelman, Structure of the gating domain of a Ca2+-activated K+ channel complexed with Ca2+/calmodulin, Nature 410 (2001) 1120–1124.

[118] M.A. Schumacher, M. Crum, M.C. Miller, Crystal structures of apocalmodulin and an apocalmodulin/SK potassium channel gating domain complex, Structure 12 (2004) 849–860.

[119] M. Zhang, C. Abrams, L. Wang, A. Gizzi, L. He, R. Lin, Y. Chen, P.J. Loll, J.M. Pascal, J.F. Zhang, Structural basis for calmodulin as a dynamic calcium sensor, Structure 20 (2012) 911–923.

[120] J.L. Fallon, M.R. Baker, L. Xiong, R.E. Loy, G. Yang, R.T. Dirksen, S.L. Hamilton, F.A. Quiocho, Crystal structure of dimeric cardiac L-type calcium channel regulatory domains bridged by Ca2+* calmodulins, Proc. Natl. Acad. Sci. U. S. A. 106 (2009) 5135–5140.

[121] E.Y. Kim, C.H. Rumpf, F. Van Petegem, R.J. Arant, F. Findeisen, E.S. Cooley, E.Y. Isacoff, D.L. Minor Jr., Multiple C-terminal tail Ca(2+)/CaMs regulate Ca(V)1.2 function but do not mediate channel dimerization, EMBO J. 29 (2010) 3924–3938.

[122] P.J. Adams, M. Ben-Johny, I.E. Dick, T. Inoue, D.T. Yue, Apocalmodulin itself promotes ion channel opening and ca(2+) regulation, Cell 159 (2014) 608–622.

[123] M.W. Berchtold, R. Egli, J.A. Rhyner, H. Hameister, E.E. Strehler, Localization of the human bona fide calmodulin genes CALM1, CALM2, and CALM3 to chromosomes 14q24-q31, 2p21.1-p21.3, and 19q13.2-q13.3, Genomics 16 (1993) 461–465.

[124] M. Nyegaard, M.T. Overgaard, M.T. Sondergaard, M. Vranas, E.R. Behr, L.L. Hildebrandt, J. Lund, P.L. Hedley, A.J. Camm, G. Wettrell, I. Fosdal, M. Christiansen, A.D. Borglum, Mutations in calmodulin cause ventricular tachycardia and sudden cardiac death, Am. J. Hum. Genet. 91 (2012) 703–712.

[125] S.G. Priori, C. Napolitano, N. Tiso, M. Memmi, G. Vignati, R. Bloise, V. Sorrentino, G.A. Danieli, Mutations in the cardiac ryanodine receptor gene (hRyR2) underlie catecholaminergic polymorphic ventricular tachycardia, Circulation 103 (2001) 196–200.

[126] L. Crotti, C.N. Johnson, E. Graf, G.M. De Ferrari, B.F. Cuneo, M. Ovadia, J. Papagiannis, M.D. Feldkamp, S.G. Rathi, J.D. Kunic, M. Pedrazzini, T. Wieland, P. Lichtner, B.M. Beckmann, T. Clark, C. Shaffer, D.W. Benson, S. Kaab, T. Meitinger, T.M. Strom, W.J. Chazin, P.J. Schwartz, A.L. George Jr., Calmodulin mutations associated with recurrent cardiac arrest in infants, Circulation 127 (2013) 1009–1017.

[127] J.R. Giudicessi, M.J. Ackerman, Potassium-channel mutations and cardiac arrhythmias–diagnosis and therapy, Nat. Rev. Cardiol. 9 (2012) 319–332.

[128] Y. Ruan, N. Liu, S.G. Priori, Sodium channel mutations and arrhythmias, Nat. Rev. Cardiol. 6 (2009) 337–348.

[129] N. Makita, N. Yagihara, L. Crotti, C.N. Johnson, B.M. Beckmann, M.S. Roh, D. Shigemizu, P. Lichtner, T. Ishikawa, T. Aiba, T. Homfray, E.R. Behr, D. Klug, I. Denjoy, E. Mastantuono, D. Theisen, T. Tsunoda, W. Satake, T. Toda, H. Nakagawa, Y. Tsuji, T. Tsuchiya, H. Yamamoto, Y. Miyamoto, N. Endo, A. Kimura, K. Ozaki, H. Motomura, K. Suda, T. Tanaka, P.J. Schwartz, T. Meitinger, S. Kaab, P. Guicheney, W. Shimizu, Z.A. Bhuiyan, H. Watanabe, W.J. Chazin, A.L. George Jr., Novel calmodulin mutations associated with congenital arrhythmia susceptibility, Circ. Cardiovasc. Genet. 7 (2014) 466–474.

[130] G.J. Reed, N.J. Boczek, S.P. Etheridge, M.J. Ackerman, CALM3 mutation associated with long QT syndrome, Heart Rhythm 12 (2015) 419–422.

[131] H.S. Hwang, F.R. Nitu, Y. Yang, K. Walweel, L. Pereira, C.N. Johnson, M. Faggioni, W.J. Chazin, D. Laver, A.L. George Jr., R.L. Cornea, D.M. Bers, B.C. Knollmann, Divergent regulation of ryanodine receptor 2 calcium release channels by arrhythmogenic human calmodulin missense mutants, Circ. Res. 114 (2014) 1114–1124.

[132] R.F. Marsman, J. Barc, L. Beekman, M. Alders, D. Dooijes, A. van den Wijngaard, I. Ratbi, A. Sefiani, Z.A. Bhuiyan, A.A. Wilde, C.R. Bezzina, A mutation in CALM1 encoding calmodulin in familial idiopathic ventricular fibrillation in childhood and adolescence, J. Am. Coll. Cardiol. 63 (2014) 259–266.

[133] H. Okano, M.S. Cyert, Y. Ohya, Importance of phenylalanine residues of yeast calmodulin for target binding and activation, J. Biol. Chem. 273 (1998) 26375–26382.

[134] A.B. Sorensen, M.T. Sondergaard, M.T. Overgaard, Calmodulin in a heartbeat, FEBS J. 280 (2013) 5511–5532.

[135] N. Chopra, B.C. Knollmann, Genetics of sudden cardiac death syndromes, Curr. Opin. Cardiol. 26 (2011) 196–203.

[136] X. Xu, M. Yano, H. Uchinoumi, A. Hino, T. Suetomi, M. Ono, H. Tateishi, T. Oda, S. Okuda, M. Doi, S. Kobayashi, T. Yamamoto, Y. Ikeda, N. Ikemoto, M. Matsuzaki, Defective calmodulin binding to the cardiac ryanodine receptor plays a key role in CPVT-associated channel dysfunction, Biochem. Biophys. Res. Commun. 394 (2010) 660–666.

[137] M. Samso, T. Wagenknecht, Apocalmodulin and Ca2+-calmodulin bind to neighboring locations on the ryanodine receptor, J. Biol. Chem. 277 (2002) 1349–1353.

[138] D.M. Balshaw, L. Xu, N. Yamaguchi, D.A. Pasek, G. Meissner, Calmodulin binding and inhibition of cardiac muscle calcium release channel (ryanodine receptor), J. Biol. Chem. 276 (2001) 20144–20153.

[139] H. Zhang, J.Z. Zhang, C.I. Danila, S.L. Hamilton, A noncontiguous, intersubunit binding site for calmodulin on the skeletal muscle Ca2+ release channel, J. Biol. Chem. 278 (2003) 8348–8355.

[140] L.W. Xiong, R.A. Newman, G.G. Rodney, O. Thomas, J.Z. Zhang, A. Persechini, M.A. Shea, S.L. Hamilton, Lobe-dependent regulation of ryanodine receptor type 1 by calmodulin, J. Biol. Chem. 277 (2002) 40862–40870.
[141] W.B. Limpitikul, I.E. Dick, R. Joshi-Mukherjee, M.T. Overgaard, A.L. George Jr., D.T. Yue, Calmodulin mutations associated with long QT syndrome prevent inactivation of cardiac L-type Ca(2+) currents and promote proarrhythmic behavior in ventricular myocytes, J. Mol. Cell. Cardiol. 74 (2014) 115–124.
[142] M.G. Erickson, B.A. Alseikhan, B.Z. Peterson, D.T. Yue, Preassociation of calmodulin with voltage-gated Ca(2+) channels revealed by FRET in single living cells, Neuron 31 (2001) 973–985.
[143] G. Yin, F. Hassan, A.R. Haroun, L.L. Murphy, L. Crotti, P.J. Schwartz, A.L. George, J. Satin, Arrhythmogenic calmodulin mutations disrupt intracellular cardiomyocyte Ca2+ regulation by distinct mechanisms, J. Am. Heart Assoc. 3 (2014) e000996.
[144] N.J. Boczek, M.L. Will, C.G. Lopocaro, D.J. Tester, M.J. Ackerman, Abstract 14699: spectrum and prevalence of CALM1, CALM2, and CALM3 mutations in long QT syndrome, catecholaminergic polymorphic ventricular tachycardia, idiopathic ventricular fibrillation, and sudden unexplained death in the Young, Circulation 128 (2013).
[145] I.A. Prior, P.D. Lewis, C. Mattos, A comprehensive survey of Ras mutations in cancer, Cancer Res. 72 (2012) 2457–2467.
[146] C. Lopez-Alcala, B. Alvarez-Moya, P. Villalonga, M. Calvo, O. Bachs, N. Agell, Identification of essential interacting elements in K-Ras/calmodulin binding and its role in K-Ras localization, J. Biol. Chem. 283 (2008) 10621–10631.
[147] P. Bhagatji, R. Leventis, R. Rich, C.J. Lin, J.R. Silvius, Multiple cellular proteins modulate the dynamics of K-ras association with the plasma membrane, Biophys. J. 99 (2010) 3327–3335.
[148] S.J. Abraham, R.P. Nolet, R.J. Calvert, L.M. Anderson, V. Gaponenko, The hypervariable region of K-Ras4B is responsible for its specific interactions with calmodulin, Biochemistry 48 (2009) 7575–7583.
[149] R.S. Sidhu, R.R. Clough, R.P. Bhullar, Ca2+/calmodulin binds and dissociates K-RasB from membrane, Biochem. Biophys. Res. Commun. 304 (2003) 655–660.
[150] M. Fivaz, T. Meyer, Reversible intracellular translocation of KRas but not HRas in hippocampal neurons regulated by Ca2+/calmodulin, J. Cell Biol. 170 (2005) 429–441.
[151] J.F. Hancock, H. Paterson, C.J. Marshall, A polybasic domain or palmitoylation is required in addition to the CAAX motif to localize p21ras to the plasma membrane, Cell 63 (1990) 133–139.
[152] J.R. Silvius, P. Bhagatji, R. Leventis, D. Terrone, K-ras4B and prenylated proteins lacking “second signals” associate dynamically with cellular membranes, Mol. Biol. Cell 17 (2006) 192–202.
[153] T.G. Bivona, S.E. Quatela, B.O. Bodemann, I.M. Ahearn, M.J. Soskis, A. Mor, J. Miura, H.H. Wiener, L. Wright, S.G. Saba, D. Yim, A. Fein, I. Perez de Castro, C. Li, C.B. Thompson, A.D. Cox, M.R. Philips, PKC regulates a farnesyl-electrostatic switch on K-Ras that promotes its association with Bcl-XL on mitochondria and induces apoptosis, Mol. Cell 21 (2006) 481–493.
[154] P.J. Sung, F.D. Tsai, H. Vais, H. Court, J. Yang, N. Fehrenbacher, J.K. Foskett, M.R. Philips, Phosphorylated K-Ras limits cell survival by blocking Bcl-xL sensitization of inositol trisphosphate receptors, Proc. Natl. Acad. Sci. U. S. A. 110 (2013) 20593–20598.
[155] B. Alvarez-Moya, C. Barcelo, F. Tebar, M. Jaumot, N. Agell, CaM interaction and Ser181 phosphorylation as new K-Ras signaling modulators, Small GTPases 2 (2011) 99–103.
[156] M. Matsubara, T. Nakatsu, H. Kato, H. Taniguchi, Crystal structure of a myristoylated CAP-23/NAP-22 N-terminal domain complexed with Ca2+/calmodulin, EMBO J. 23 (2004) 712–718.
[157] M. Matsubara, K. Titani, H. Taniguchi, N. Hayashi, Direct involvement of protein myristoylation in myristoylated alanine-rich C kinase substrate (MARCKS)-calmodulin interaction, J. Biol. Chem. 278 (2003) 48898–48902.
[158] S.L. Zhang, Y. Yu, J. Roos, J.A. Kozak, T.J. Deerinck, M.H. Ellisman, K.A. Stauderman, M.D. Cahalan, STIM1 is a Ca2+ sensor that activates CRAC channels and migrates from the Ca2+ store to the plasma membrane, Nature 437 (2005) 902–905.
[159] O. Mignen, J.L. Thompson, T.J. Shuttleworth, Orai1 subunit stoichiometry of the mammalian CRAC channel pore, J. Physiol. 586 (2008) 419–425.
[160] M. Vig, A. Beck, J.M. Billingsley, A. Lis, S. Parvez, C. Peinelt, D.L. Koomoa, J. Soboloff, D.L. Gill, A. Fleig, J.P. Kinet, R. Penner, CRACM1 multimers form the ion-selective pore of the CRAC channel, Curr. Biol. 16 (2006) 2073–2079.
[161] M. Vig, C. Peinelt, A. Beck, D.L. Koomoa, D. Rabah, M. Koblan-Huberson, S. Kraft, H. Turner, A. Fleig, R. Penner, J.P. Kinet, CRACM1 is a plasma membrane protein essential for store-operated Ca2+ entry, Science 312 (2006) 1220–1223.
[162] A.V. Yeromin, S.L. Zhang, W. Jiang, Y. Yu, O. Safrina, M.D. Cahalan, Molecular identification of the CRAC channel by altered ion selectivity in a mutant of Orai, Nature 443 (2006) 226–229.
[163] T. Hewavitharana, X. Deng, J. Soboloff, D.L. Gill, Role of STIM and Orai proteins in the store-operated calcium signaling pathway, Cell Calcium 42 (2007) 173–182.
[164] J.C. Mercer, W.I. Dehaven, J.T. Smyth, B. Wedel, R.R. Boyles, G.S. Bird, J.W. Putney Jr., Large store-operated calcium-selective currents due to co-expression of Orai1 or Orai2 with the intracellular calcium sensor, Stim1, J. Biol. Chem. 281 (2006) 24979–24990.
[165] A. Berna-Erro, A. Braun, R. Kraft, C. Kleinschnitz, M.K. Schuhmann, D. Stegner, T. Wultsch, J. Eilers, S.G. Meuth, G. Stoll, B. Nieswandt, STIM2 regulates capacitive Ca2+ entry in neurons and plays a key role in hypoxic neuronal cell death, Sci. Signal. 2 (2009) ra67.
[166] O. Brandman, J. Liou, W.S. Park, T. Meyer, STIM2 is a feedback regulator that stabilizes basal cytosolic and endoplasmic reticulum Ca2+ levels, Cell 131 (2007) 1327–1339.
[167] R.M. Luik, B. Wang, M. Prakriya, M.M. Wu, R.S. Lewis, Oligomerization of STIM1 couples ER calcium depletion to CRAC channel activation, Nature 454 (2008) 538–542.
[168] P.B. Stathopulos, G.Y. Li, M.J. Plevin, J.B. Ames, M. Ikura, Stored Ca2+ depletion-induced oligomerization of stromal interaction molecule 1 (STIM1) via the EF-SAM region: an initiation mechanism for capacitive Ca2+ entry, J. Biol. Chem. 281 (2006) 35855–35862.
[169] M. Muik, I. Frischauf, I. Derler, M. Fahrner, J. Bergsmann, P. Eder, R. Schindl, C. Hesch, B. Polzinger, R. Fritsch, H. Kahr, J. Madl, H. Gruber, K. Groschner, C. Romanin, Dynamic coupling of the putative coiled-coil domain of ORAI1 with STIM1 mediates ORAI1 channel activation, J. Biol. Chem. 283 (2008) 8014–8022.
[170] C.Y. Park, P.J. Hoover, F.M. Mullins, P. Bachhawat, E.D. Covington, S. Raunser, T. Walz, K.C. Garcia, R.E. Dolmetsch, R.S. Lewis, STIM1 clusters and activates CRAC channels via direct binding of a cytosolic domain to Orai1, Cell 136 (2009) 876–890.
[171] J.P. Yuan, W. Zeng, M.R. Dorwart, Y.J. Choi, P.F. Worley, S. Muallem, SOAR and the polybasic STIM1 domains gate and regulate Orai channels, Nat. Cell Biol. 11 (2009) 337–343.
[172] L. Zheng, P.B. Stathopulos, G.Y. Li, M. Ikura, Biophysical characterization of the EF-hand and SAM domain containing Ca2+ sensory region of STIM1 and STIM2, Biochem. Biophys. Res. Commun. 369 (2008) 240–246.
[173] L. Zheng, P.B. Stathopulos, R. Schindl, G.Y. Li, C. Romanin, M. Ikura, Auto-inhibitory role of the EF-SAM domain of STIM proteins in store-operated calcium entry, Proc. Natl. Acad. Sci. U. S. A. 108 (2011) 1337–1342.
[174] L. Holm, S. Kaariainen, C. Wilton, D. Plewczynski, Using Dali for structural comparison of proteins, Curr. Protoc. Bioinform. Chapter 5 (2006). Unit 5 5.
[175] C.D. Thanos, K.E. Goodwill, J.U. Bowie, Oligomeric structure of the human EphB2 receptor SAM domain, Science 283 (1999) 833–836.
[176] F. Qiao, J.U. Bowie, The many faces of SAM, Sci. STKE 2005 (2005) re7.
[177] Y. Baba, K. Hayashi, Y. Fujii, A. Mizushima, H. Watarai, M. Wakamori, T. Numaga, Y. Mori, M. Iino, M. Hikida, T. Kurosaki, Coupling of STIM1 to store-operated Ca2+ entry through its constitutive and inducible movement in the endoplasmic reticulum, Proc. Natl. Acad. Sci. U. S. A. 103 (2006) 16704–16709.
[178] E.D. Covington, M.M. Wu, R.S. Lewis, Essential role for the CRAC activation domain in store-dependent oligomerization of STIM1, Mol. Biol. Cell 21 (2010) 1897–1907.
[179] Y. Furukawa, S. Teraguchi, T. Ikegami, O. Dagliyan, L. Jin, D. Hall, N.V. Dokholyan, K. Namba, S. Akira, T. Kurosaki, Y. Baba, D.M. Standley, Intrinsic disorder mediates cooperative signal transduction in STIM1, J. Mol. Biol. 426 (2014) 2082–2097.
[180] Y. Zhou, P. Srinivasan, S. Razavi, S. Seymour, P. Meraner, A. Gudlur, P.B. Stathopulos, M. Ikura, A. Rao, P.G. Hogan, Initial activation of STIM1, the regulator of store-operated calcium entry, Nat. Struct. Mol. Biol. 20 (2013) 973–981.
[181] P. Malaney, R.R. Pathak, B. Xue, V.N. Uversky, V. Dave, Intrinsic disorder in PTEN and its interactome confers structural plasticity and functional versatility, Sci. Rep. 3 (2013) 2035.
[182] A.B. Sigalov, V.N. Uversky, Differential occurrence of protein intrinsic disorder in the cytoplasmic signaling domains of cell receptors, Self Nonself 2 (2011) 55–72.
[183] A.V. Uversky, B. Xue, Z. Peng, L. Kurgan, V.N. Uversky, On the intrinsic disorder status of the major players in programmed cell death pathways, F1000Res. 2 (2013) 190.
[184] P.E. Wright, H.J. Dyson, Linking folding and binding, Curr. Opin. Struct. Biol. 19 (2009) 31–38.
[185] B. Xue, A.K. Dunker, V.N. Uversky, The roles of intrinsic disorder in orchestrating the Wnt-pathway, J. Biomol. Struct. Dyn. 29 (2012) 843–861.
[186] J. Liou, M. Fivaz, T. Inoue, T. Meyer, Live-cell imaging reveals sequential oligomerization and local plasma membrane targeting of stromal interaction molecule 1 after Ca2+ store depletion, Proc. Natl. Acad. Sci. U. S. A. 104 (2007) 9301–9306.
[187] R.M. Luik, M.M. Wu, J. Buchanan, R.S. Lewis, The elementary unit of store-operated Ca2+ entry: local activation of CRAC channels by STIM1 at ER-plasma membrane junctions, J. Cell Biol. 174 (2006) 815–825.
[188] M.M. Wu, J. Buchanan, R.M. Luik, R.S. Lewis, Ca2+ store depletion causes STIM1 to accumulate in ER regions closely associated with the plasma membrane, J. Cell Biol. 174 (2006) 803–813.
[189] M. Muik, M. Fahrner, I. Derler, R. Schindl, J. Bergsmann, I. Frischauf, K. Groschner, C. Romanin, A cytosolic homomerization and a modulatory domain within STIM1 C terminus determine coupling to ORAI1 channels, J. Biol. Chem. 284 (2009) 8421–8426.
[190] M. Muik, M. Fahrner, R. Schindl, P. Stathopulos, I. Frischauf, I. Derler, P. Plenk, B. Lackner, K. Groschner, M. Ikura, C. Romanin, STIM1 couples to ORAI1 via an intramolecular transition into an extended conformation, EMBO J. 30 (2011) 1678–1689.
[191] N. Calloway, T. Owens, K. Corwith, W. Rodgers, D. Holowka, B. Baird, Stimulated association of STIM1 and Orai1 is regulated by the balance of PtdIns(4,5)P(2) between distinct membrane pools, J. Cell Sci. 124 (2011) 2602–2610.

[192] M.K. Korzeniowski, M.A. Popovic, Z. Szentpetery, P. Varnai, S.S. Stojilkovic, T. Balla, Dependence of STIM1/Orai1-mediated calcium entry on plasma membrane phosphoinositides, J. Biol. Chem. 284 (2009) 21027–21035.
[193] C.M. Walsh, M. Chvanov, L.P. Haynes, O.H. Petersen, A.V. Tepikin, R.D. Burgoyne, Role of phosphoinositides in STIM1 dynamics and store-operated calcium entry, Biochem. J. 425 (2010) 159–168.
[194] X. Hou, L. Pedi, M.M. Diver, S.B. Long, Crystal structure of the calcium release-activated calcium channel Orai, Science 338 (2012) 1308–1313.
[195] P.B. Stathopulos, R. Schindl, M. Fahrner, L. Zheng, G.M. Gasmi-Seabrook, M. Muik, C. Romanin, M. Ikura, STIM1/Orai1 coiled-coil interplay in the regulation of store-operated calcium entry, Nat. Commun. 4 (2013) 2963.
[196] B. Cui, X. Yang, S. Li, Z. Lin, Z. Wang, C. Dong, Y. Shen, The inhibitory helix controls the intramolecular conformational switching of the C-terminus of STIM1, PLoS One 8 (2013) e74735.
[197] X. Yang, H. Jin, X. Cai, S. Li, Y. Shen, Structural and mechanistic insights into the activation of Stromal interaction molecule 1 (STIM1), Proc. Natl. Acad. Sci. U. S. A. 109 (2012) 5657–5662.
[198] M. Fahrner, M. Muik, R. Schindl, C. Butorac, P. Stathopulos, L. Zheng, I. Jardin, M. Ikura, C. Romanin, A coiled-coil clamp controls both conformation and clustering of stromal interaction molecule 1 (STIM1), J. Biol. Chem. 289 (2014) 33231–33244.
[199] P.J. Shaw, B. Qu, M. Hoth, S. Feske, Molecular regulation of CRAC channels and their role in lymphocyte function, Cell. Mol. Life Sci. 70 (2013) 2637–2656.
[200] P.B. Stathopulos, M. Ikura, Structure and function of endoplasmic reticulum STIM calcium sensors, Curr. Top. Membr. 71 (2013) 59–93.
[201] P.B. Stathopulos, L. Zheng, M. Ikura, Stromal interaction molecule (STIM) 1 and STIM2 calcium sensing regions exhibit distinct unfolding and oligomerization kinetics, J. Biol. Chem. 284 (2009) 728–732.
[202] S. Feske, Y. Gwack, M. Prakriya, S. Srikanth, S.H. Puppel, B. Tanasa, P.G. Hogan, R.S. Lewis, M. Daly, A. Rao, A mutation in Orai1 causes immune deficiency by abrogating CRAC channel function, Nature 441 (2006) 179–185.
[203] W. Bergmeier, C. Weidinger, I. Zee, S. Feske, Emerging roles of store-operated Ca(2)(+) entry through STIM and ORAI proteins in immunity, hemostasis and cancer, Channels (Austin) 7 (2013) 379–391.
[204] S. Feske, ORAI1 and STIM1 deficiency in human and mice: roles of store-operated Ca2+ entry in the immune system and beyond, Immunol. Rev. 231 (2009) 189–209.
[205] F. Le Deist, C. Hivroz, M. Partiseti, C. Thomas, H.A. Buc, M. Oleastro, B. Belohradsky, D. Choquet, A. Fischer, A primary T-cell immunodeficiency associated with defective transmembrane calcium influx, Blood 85 (1995) 1053–1062.
[206] C.A. McCarl, C. Picard, S. Khalil, T. Kawasaki, J. Rother, A. Papolos, J. Kutok, C. Hivroz, F. Ledeist, K. Plogmann, S. Ehl, G. Notheis, M.H. Albert, B.H. Belohradsky, J. Kirschner, A. Rao, A. Fischer, S. Feske, ORAI1 deficiency and lack of store-operated Ca2+ entry cause immunodeficiency, myopathy, and ectodermal dysplasia, J. Allergy Clin. Immunol. 124 (2009) 1311–1318 e1317.
[207] M. Partiseti, F. Le Deist, C. Hivroz, A. Fischer, H. Korn, D. Choquet, The calcium current activated by T cell receptor and store depletion in human lymphocytes is absent in a primary immunodeficiency, J. Biol. Chem. 269 (1994) 32327–32335.
[208] M. Byun, A. Abhyankar, V. Lelarge, S. Plancoulaine, A. Palanduz, L. Telhan, B. Boisson, C. Picard, S. Dewell, C. Zhao, E. Jouanguy, S. Feske, L. Abel, J.L. Casanova, Whole-exome sequencing-based discovery of STIM1 deficiency in a child with fatal classic Kaposi sarcoma, J. Exp. Med. 207 (2010) 2307–2312.
[209] C. Picard, C.A. McCarl, A. Papolos, S. Khalil, K. Luthy, C. Hivroz, F. LeDeist, F. Rieux-Laucat, G. Rechavi, A. Rao, A. Fischer, S. Feske, STIM1 mutation associated with a syndrome of immunodeficiency and autoimmunity, N. Engl. J. Med. 360 (2009) 1971–1980.
[210] K.T. Cheng, I. Alevizos, X. Liu, W.D. Swaim, H. Yin, S. Feske, M. Oh-hora, I.S. Ambudkar, STIM1 and STIM2 protein deficiency in T lymphocytes underlies development of the exocrine gland autoimmune disease, Sjogren's syndrome, Proc. Natl. Acad. Sci. U. S. A. 109 (2012) 14544–14549.
[211] S. Fuchs, A. Rensing-Ehl, C. Speckmann, B. Bengsch, A. Schmitt-Graeff, I. Bondzio, A. Maul-Pavicic, T. Bass, T. Vraetz, B. Strahm, T. Ankermann, M. Benson, A. Caliebe, R. Folster-Holst, P. Kaiser, R. Thimme, W.W. Schamel, K. Schwarz, S. Feske, S. Ehl, Antiviral and regulatory T cell immunity in a patient with stromal interaction molecule 1 deficiency, J. Immunol. 188 (2012) 1523–1533.
[212] D. Misceo, A. Holmgren, W.E. Louch, P.A. Holme, M. Mizobuchi, R.J. Morales, A.M. De Paula, A. Stray-Pedersen, R. Lyle, B. Dalhus, G. Christensen, H. Stormorken, G.E. Tjonnfjord, E. Frengen, A dominant STIM1 mutation causes Stormorken syndrome, Hum. Mutat. 35 (2014) 556–564.
[213] G. Morin, N.O. Bruechle, A.R. Singh, C. Knopp, G. Jedraszak, M. Elbracht, D. Bremond-Gignac, K. Hartmann, H. Sevestre, P. Deutz, D. Herent, P. Nurnberg, B. Romeo, K. Konrad, M. Mathieu-Dramard, J. Oldenburg, E. Bourges-Petit, Y. Shen, K. Zerres, H. Ouadid-Ahidouch, J. Rochette, Gain-of-Function mutation in STIM1 (P.R304W) is associated with Stormorken syndrome, Hum. Mutat. 35 (2014) 1221–1232.
[214] S.A. Forbes, D. Beare, P. Gunasekaran, K. Leung, N. Bindal, H. Boutselakis, M. Ding, S. Bamford, C. Cole, S. Ward, C.Y. Kok, M. Jia, T. De, J.W. Teague, M.R. Stratton, U. McDermott, P.J. Campbell, COSMIC: exploring the world's knowledge of somatic mutations in human cancer, Nucleic Acids Res. 43(Database issue) (2015) D805–D811.
[215] P.B. Stathopulos, M. Ikura, Structurally delineating stromal interaction molecules as the endoplasmic reticulum calcium sensors and regulators of calcium release-activated calcium entry, Immunol. Rev. 231 (2009) 113–131.
[216] M.C. Bauer, D. O'Connell, D.J. Cahill, S. Linse, Calmodulin binding to the polybasic C-termini of STIM proteins involved in store-operated calcium entry, Biochemistry 47 (2008) 6089–6091.
[217] F.M. Mullins, C.Y. Park, R.E. Dolmetsch, R.S. Lewis, STIM1 and calmodulin interact with Orai1 to induce Ca2+-dependent inactivation of CRAC channels, Proc. Natl. Acad. Sci. U. S. A. 106 (2009) 15495–15500.
[218] Y. Liu, X. Zheng, G.A. Mueller, M. Sobhany, E.F. DeRose, Y. Zhang, R.E. London, L. Birnbaumer, Crystal structure of calmodulin binding domain of orai1 in complex with Ca2+ calmodulin displays a unique binding mode, J. Biol. Chem. 287 (2012) 43030–43041.
[219] B.J. Marsden, G.S. Shaw, B.D. Sykes, Calcium binding proteins. Elucidating the contributions to calcium affinity from an analysis of species variants and peptide fragments, Biochem. Cell Biol. 68 (1990) 587–601.